

AD _____

Award Number: DAMD17-02-1-0111

TITLE: Prevention of Development of Recurrent Growth
of Prostate Cancer

PRINCIPAL INVESTIGATOR: James L. Mohler, M.D.

CONTRACTING ORGANIZATION: University of North Carolina
Chapel Hill, North Carolina 27599-1350

REPORT DATE: February 2003

TYPE OF REPORT: Annual

PREPARED FOR: U.S. Army Medical Research and Materiel Command
Fort Detrick, Maryland 21702-5012

DISTRIBUTION STATEMENT: Approved for Public Release;
Distribution Unlimited

The views, opinions and/or findings contained in this report are those of the author(s) and should not be construed as an official Department of the Army position, policy or decision unless so designated by other documentation.

20030702 046

REPORT DOCUMENTATION PAGE			Form Approved OMB No. 074-0188	
Public reporting burden for this collection of information is estimated to average 1 hour per response, including the time for reviewing instructions, searching existing data sources, gathering and maintaining the data needed, and completing and reviewing this collection of information. Send comments regarding this burden estimate or any other aspect of this collection of information, including suggestions for reducing this burden to Washington Headquarters Services, Directorate for Information Operations and Reports, 1215 Jefferson Davis Highway, Suite 1204, Arlington, VA 22202-4302, and to the Office of Management and Budget, Paperwork Reduction Project (0704-0188), Washington, DC 20503				
1. AGENCY USE ONLY (Leave blank)	2. REPORT DATE February 2003	3. REPORT TYPE AND DATES COVERED Annual (1 Feb 02 - 31 Jan 03)		
4. TITLE AND SUBTITLE Prevention of Development of Recurrent Growth of Prostate Cancer		5. FUNDING NUMBERS DAMD17-02-1-0111		
6. AUTHOR(S) James L. Mohler, M.D.				
7. PERFORMING ORGANIZATION NAME(S) AND ADDRESS(ES) University of North Carolina Chapel Hill, North Carolina 27599-1350 E-Mail: jmhohler@med.unc.edu		8. PERFORMING ORGANIZATION REPORT NUMBER		
9. SPONSORING / MONITORING AGENCY NAME(S) AND ADDRESS(ES) U.S. Army Medical Research and Materiel Command Fort Detrick, Maryland 21702-5012		10. SPONSORING / MONITORING AGENCY REPORT NUMBER		
11. SUPPLEMENTARY NOTES Original contains color plates. All DTIC reproductions will be in black and white.				
12a. DISTRIBUTION / AVAILABILITY STATEMENT Approved for Public Release; Distribution Unlimited			12b. DISTRIBUTION CODE	
13. ABSTRACT (Maximum 200 Words) The purpose of the proposed studies is to identify and then target one gene or a small number of genes critical for the development of recurrent growth of CaP. Differential expression analysis, subtractive hybridization and immunohistochemistry were used in the androgen-dependent human prostate cancer CWR22 model to identify 10 genes whose expression might be associated with the onset of CaP recurrence. In the first year of the proposed studies, we have visually scored 8 gene proteins in CWR22 tumors on day 120 after castration and identified Nkx3.1, α -tubulin and IGFBP-5 as potential targets. In order to more rigorously test these gene targets, we developed a hybrid immunostaining protocol for comparison of expression of antigens in proliferating versus non-proliferating cells. We have collected the necessary reagents (BrdU-labeled tumors), are modifying our image analysis algorithms to allow quantitation, have demonstrated the feasibility of an antisense approach and have begun to work with the serial prostate biopsies. We have made progress toward identifying targets for antisense therapy that will be tested in <i>in vitro</i> in CaP cell lines and <i>in vivo</i> in the CWR22 model.				
14. SUBJECT TERMS Recurrent Prostate Cancer, Gene Therapy			15. NUMBER OF PAGES 40	
			16. PRICE CODE	
17. SECURITY CLASSIFICATION OF REPORT Unclassified	18. SECURITY CLASSIFICATION OF THIS PAGE Unclassified	19. SECURITY CLASSIFICATION OF ABSTRACT Unclassified	20. LIMITATION OF ABSTRACT Unlimited	

Table of Contents

Cover.....	1
SF 298.....	2
Table of Contents.....	3
Introduction.....	4
Body.....	4
Key Research Accomplishments.....	11
Reportable Outcomes.....	12
Conclusions.....	12
References.....	12
Appendices.....	13

INTRODUCTION

The subject of the proposed studies is the poor performance of androgen deprivation therapy for advanced prostate cancer (CaP). The purpose of the proposed studies is to identify and then target one gene or a small number of genes critical for the development of recurrent growth of CaP. In order to accomplish this goal, we used the human CaP xenograft, CWR22. CWR22 retains the biological characteristics exhibited by most human CaP- tumor regression after castration and tumor recurrence approximately 5 months later (recurrent CWR22). Differential expression analysis and subtractive hybridization were used to identify transcripts expressed in intact mice bearing CWR22 tumors and castrated mice bearing recurrent CWR22 tumors but *not in regressed tumors*. Northern and western analyses were used to confirm temporal association with tumor growth before and after castration. Genes identified included 6 androgen-regulated genes [human kallikrein type 2 (hK2), Nkx3.1, insulin-like growth factor binding protein-5 (IGFBP-5), α -tubulin, α -enolase and thioredoxin-binding protein 2 (TBP2)] and 4 androgen-*unregulated* genes [tomoregulin, a novel EGF-like molecule, translation elongation factor-1 α (EF-1 α), Mxi1 and an unknown gene]. Immunohistochemistry was used to recognize small foci of 5-20 proliferating cells that became apparent on day 120 after castration. These foci of proliferating cells immunostained for androgen receptor (AR) and increased levels of prostate specific antigen (PSA), an androgen receptor regulated gene product. The appearance of proliferating tumor cells that expressed AR and PSA 120 days after castration suggests that these cells represent the origin of recurrent CaP. We created tissue microarrays of CWR22 tumors (intact, recurrent and from multiple intervals after castration) that were immunostained with antibodies against tomoregulin, EF-1 α and thioredoxin reductase-1 (TR-1), a member of the TBP2 gene family. All 3 genes were expressed on day 120 after castration, intact CWR22 and recurrent CWR22 but *not in regressed tumors*.

BODY

Aim 1) Complete the identification of genes that are associated with the onset of cell proliferation after castration in the CWR22 model

Overview: In Aim 1, the expression of the candidate genes will be correlated temporally with cell proliferation and compared directly in Ki-67+ and Ki-67- cells at the precise onset of recurrent proliferation using a full range of immunohistochemical techniques in the CWR22 tumor model.

- Characterize the expression of candidate genes identified using differential expression analysis and subtractive hybridization in the CWR22 model using automated image analysis of immunohistochemical preparations of CWR22 tissue microarrays (months 1-12)

At the time of proposal submission, the CWR22 tissue micro arrays had been immunostained for Ki-67, tomoregulin, EF1 α and thioredoxin reductase-1 (TR-1). The manuscript describing our work that formed the basis for the proposal included these genes of interest as well as Mxi-1. Since, we have immunostained the tissue microarrays for Nkx3.1, IGFBP-5, α -tubulin, non-neuronal enolase (NNE) and 14-3-3 η . We are in the process of immunostaining for hK2, CEA and ARA-70. Since image analyzing the tissue microarrays takes so long, we have focused upon assessing the time-points after castration that represent the onset of androgen-independent growth (days 90, 100, 110 and 120 after castration) and the development of a method that allows direct comparison of antigen expression in of proliferating versus non-proliferating cells.

The immunohistochemical evaluation of genes of potential interest continues as described in the table below. The table describes our overall progress in securing antibodies, completing immunohistochemical staining of adjacent sections at the onset of cellular proliferation after castration, visual scoring of **foci** of proliferating versus non-proliferating cells in **adjacent sections**, dual labeling using standard (immunoperoxidase) and fluorescent (anti-BrdU) immunohistochemistry for quantitative image analysis of **individual** proliferating versus non-proliferating cells **in the same section**. Genes of interest include those implicated by differential expression analysis or subtractive hybridization described in the grant application (D1-10), other genes uncovered by subtractive hybridization (M1-5) or differential expression analysis (G1) but deemed unlikely to be significant and 14-3-3 η that appears unlikely to be significant. 14-3-3 proteins are a family of homo or heterodimeric α -helical proteins that interact with a diverse number of target proteins, including kinases, phosphatases, enzymes, transcription factors and non-kinase receptors (Wakui, 1997; Fu, 2000). We have characterized the interaction of human AR and 14-3-3 η protein, and 14-3-3 η expression and location in human CaP and CWR22 xenograft tumors. Our results indicate that AR is a target protein for 14-3-3 η and suggest a possible mechanism for cross-talk with intracellular signaling pathways or modification of AR function in recurrent CaP.

#	Name	Source	Ab	Visually Scored	Correlation	Dual Label	Image Analysis
D1	hK2	Mayo	Mouse MAb	In Progress			
D2	Nkx3.1	Santa Cruz	Goat PAb	Y	Y	Y	Y
D3	IGFBP-5	Santa Cruz	Goat PAb	Y	Y		
D4	alpha-tubulin	ABCAM	Rat MAb	Y	Y		
D5	NNE	Accurate Chemical	Rabbit PAb	Y	N		
	enolase (α , β and γ)	Santa Cruz	Goat PAb	--	--	--	--
D6	TR-1	Upstate	Rabbit PAb	Y	N		
D7	Tomoregulin	Sakamoto Lab	Mouse MAb	Y	N		
D8	EF-1 α	Upstate	Mouse MAb	In Progress			
D9	MXI-1	BD Pharmigen	Mouse MAb	Y	N		

D10	HSA36	N/A	--	--	--	--	--
T1	14-3-3 η	Santa Cruz	Goat PAb	Y	N		

Adjacent sections immunostained for Ki-67 to identify foci of cellular proliferation and the gene product of interest were scored visually. Five fields of view containing 20 cells were scored for proliferating and non-proliferating areas of each tumor specimen. Each cell was scored from 0 (no immunostaining) to 3 (intense immunostaining) yielding a total score ranging from 0-300 for each tumor area. The tumor visual scores were expressed as the visual score out of 300 and as a fraction of 1 for ease of comparison. For TR-1, 5 fields of views (FOV) corresponding to regions of low cellular proliferation were not available for scoring. The complete process for obtaining a visual score was performed twice for each tumor. The visual scores appeared most interesting for α -Tubulin, IGFBP-5 and Nkx3.1 (bolded in table below).

DOD Project Visual Scores					
Gene Product	CWR22 Tumor Evaluated	Low Proliferation		High Proliferation	
14-3-3 η	120dCx	177/300	0.59	213/300	0.71
		223/300	0.74	229/300	0.76
α -Tubulin	120dCx	132/300	0.44	231/300	0.77
		172/300	0.57	249/300	0.83
IGFBP-5	120dCx	127/300	0.42	181/300	0.60
		72/300	0.24	156/300	0.52
Mxi-1	120dCx	152/300	0.51	193/300	0.64
		213/300	0.71	184/300	0.61
Nkx3.1	120dCx	110/300	0.37	170/300	0.57
		147/300	0.49	229/300	0.76
NNE	120dCx	135/300	0.45	198/300	0.66
		186/300	0.62	179/300	0.60
TR-1	120dCx	139/300	0.46	38/120	0.32
		83/300	0.28	28/120	0.23
Tomoregulin	105dCx	52/300	0.17	121/300	0.40
		203/300	0.68	185/300	0.62

- Confirm the association of candidate genes with the onset of androgen-independent proliferation using immunostaining to compare expression in proliferating (Ki-67 positive) versus non-proliferating (Ki-67 negative) cells in CWR22 tumors 120 days after castration (months 1-12)

Initial evaluation of the correlation of gene product expression with cellular proliferation was achieved using standard immunohistochemical techniques to label serially cut sections of formalin-fixed, paraffin-embedded CWR22 human prostate cancer xenografts. Immunodetection of four gene products (EF-1 α , hk2, Mxi-1 and tomoregulin) required modifying the standard protocol by using the Vector Mouse on Mouse Kit. Six-micrometer sections were

deparaffinized and rehydrated using Hemo-De and graded alcohols. Immunodetection of gene products and Ki-67 (a proliferation marker) was performed using either the Protocol™ MicroProbe staining system (α -tubulin, 14-3-3 η , hk2, Nkx3.1 and Ki-67) (Fisher Scientific) or a tape transfer protocol (EF-1 α , MXI-1, α -enolase, IGFBP-5, tomoregulin and TR-1) (Instrumedics). Antigens were retrieved by incubation in citrate buffer (pH 6.0; Biocare Medical) for 2 minutes at 120°C and approximately 22 psi. Endogenous peroxidases were blocked using 3% H₂O₂ followed by incubations using 5% normal serum and an avidin-biotin blocking reagent (Vector Labs) each for 15 minutes at 37°C. Specimens were incubated for one hour at 37°C with anti-human primary antibodies created against the gene products of interest. Tissues were incubated with biotinylated secondary antibodies (Vector Labs) followed by avidin-biotin complex (Vector Labs). The complex was visualized using 3, 3'-diaminobenzidine (DAB) (Vector Labs). Counterstaining was performed using hematoxylin (Gill's formula; Vector Labs).

In order to make direct comparison of antigen expression in proliferating versus non-proliferating cells, we have spent 7 years evaluating different approaches. Our goal was an immunostaining protocol that allows for the dual labeling of either Ki-67 or 5-bromo-2-deoxyuridine (BrdU) (primary label) with other antibodies of interest (second label). Each labeled epitope should be clearly resolved and the Ki-67 or BrdU label must not interfere with the quantification of the second primary of interest during image analysis. The limitations we have found and the unsuccessful approaches include the following: 1) Limited availability of antibodies of interest in terms of host species and isotypes (all antibodies of interest were of an IgG isotype) limits pairing with the mouse anti ki-67 IgG or the sheep anti BrdU IgG. This introduces the potential for secondary antibodies to recognize more than one primary antibody. A Ki-67 IgM was located and tried but produced poor results in paraffin sections. 2) The need for amplification of signal in paraffin-embedded tissue precludes direct labeling methods. Indirect labeling along with amplification steps leads to the potential for cross reactivity. 3) The use of adsorbed secondary antibodies (in this case adsorption against mouse IgG due to the presence of mouse immunoglobulins in the CRW22 human prostate cancer xenografts) usually leads to poor signal in paraffin sections due to possible loss of reactivity to certain subclasses of IgG. 4) Well-resolved probes are often not possible since epitopes may be co-localized in the cell. 5) The use of mouse primary antibodies in the CWR22 model necessitates the inclusion of a Mouse on Mouse kit (Vector Labs).

A hybrid peroxidase/fluorescent dual labeling protocol was developed in order to derive robust images for image analysis. Cell proliferation was determined using a fluorescent-labeled BrdU. The proliferating cells were identified using fluorescence that did not interfere with image analysis for the peroxidase-labeled primary. Our method is demonstrated for simultaneous assessment of proliferation and Nkx3.1 expression since Nkx3.1 expression proved most interesting when scored visually (see table above).

CWR22 specimens were BrdU-labeled prior to castration and at various times after castration to generate the biological reagents for these studies. Methods used for tumor injection, propagation, harvest and preservation were described previously (Gregory, 2001; Wainstein, 1994). Briefly, CWR22 tumors were transplanted subcutaneously into 4 to 5 week-old nude/athymic mice (Harlan Sprague-Dawley) as a suspension of 1 million cells in Matrigel™ (BD Biosciences). Two days prior to tumor injection a testosterone pellet (12.5 mg sustained-

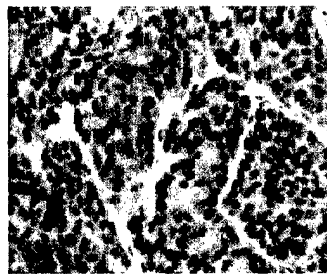
release, Innovative Research of America) was placed subcutaneously to maintain an approximate serum testosterone level of 4 ng/ml. Animals were anesthetized with methoxyflurane, castrated and testosterone pellets removed when tumors reached a volume of 1 cm³. Four hours prior to tumor harvest, the mice were injected intraperitoneally with a 10mM solution of BrdU in sterile phosphate-buffered saline (PBS). Each animal was injected with 1mL of BrdU solution per 100g of body weight. Subsequently, mice were anesthetized and sacrificed by cervical dislocation. Tumors were harvested and fixed in 10% buffered formalin for 24 to 48 hours. Fixed tumors were washed in PBS for 24 hours, dehydrated and embedded in paraffin. The Institutional Animal Care and Use Committee of the University of North Carolina at Chapel Hill approved all procedures used.

CWR22 Human Prostate Cancer Xenografts + BrdU			
Animal ID	Days after Castration (Cx)	Harvest Date	BrdU
02-119	Intact	1/27/2003	4hr
11--1	Intact	1/27/2003	4hr
02.11.4	50 dCx	2/5/2003	4hr
9--1	90 dCx	1/9/2003	4hr
9--4	90 dCx	1/9/2003	4hr
9--5	90 dCx	1/9/2003	4hr
9--6	90 dCx	1/9/2003	4hr
4	100 dCx	10/28/2002	4hr
8	100 dCx	10/28/2002	4hr
7	100 dCx	10/28/2002	4hr
6	110 dCx	10/30/2002	4hr
10	110 dCx	10/30/2002	4hr
5	120 dCx	11/19/2002	4hr
9--3	120 dCx	2/19/2003	4hr
A	Recurrent	6/6/2002	4hr
B	Recurrent	6/6/2002	4hr
C	Recurrent	6/6/2002	4hr
D	Recurrent	6/6/2002	4hr
E	Recurrent	6/6/2002	4hr

Immunodetection of gene products was the same as the peroxidase method described above for the labeling of serial sections. In addition, a second antigen retrieval was performed on the same section of tissue using Nuclear Decloaker retrieval buffer (pH9.0; Biocare Medical) for 2 minutes at 120° C and approximately 22 psi. Tissues were incubated with anti-BrdU sheep IgG (ABCAM) followed by incubation with rhodamine-conjugated donkey anti-sheep IgG F(ab')₂ fragments that had been absorbed against the IgG and serum of rabbits, mice and humans (Jackson ImmunoResearch). The sections were mounted using either Gel Mount aqueous mounting medium (Biomed) or Vectashield with DAPI (Vector Labs).

Immunoperoxidase staining revealed Nkx3.1 expression in CWR22 on day 120 after castration (top left). Rhodamine fluorescence distinguished proliferating from non-proliferating cells (bottom left). The RGB model was used to generate a threshold based on red intensity to

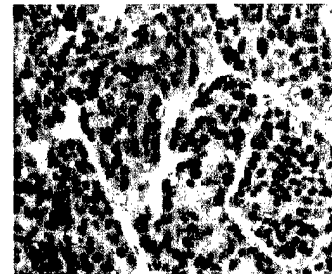
segment BrdU-positive regions within the fluorescent image. Two masks were generated from this segmentation- one masking BrdU-positive nuclei (top middle) and one masking everything other than BrdU-positive nuclei (bottom middle). These masks were added to the original immunoperoxidase image captured using light microscopy yielding two images- one exhibiting only proliferating nuclei (bottom right) and one with everything except proliferating nuclei (top right). Image analysis using ImagePro 4.5 will be modified to compare quantitatively Nkx3.1 expression in proliferating versus non-proliferating cells (Kim, 1999).



IP-IHC-Nkx3.1



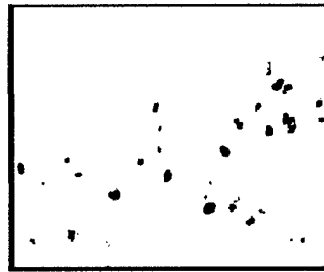
Proliferating Nuclei Mask



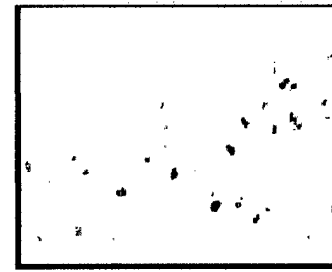
Non-proliferating Nuclei IP



BrdU-Rhodamine



Non-proliferating Nuclei Mask



Proliferating Nuclei IP

Aim 2) Correlate the expression of proliferation-associated genes identified in Aim 1 to cell proliferation using clinical specimens of androgen-stimulated and recurrent CaP and serial prostate biopsies performed before and after castration in men with advanced CaP

Overview: The expression of candidate regulatory genes found most promising in Aim 1 will be examined for over-expression in both androgen-stimulated CaP (obtained from radical prostatectomy specimens) and recurrent CaP (obtained from transurethral resection specimens from men with urinary retention due to local CaP recurrence long after androgen deprivation therapy). Over-expressed genes will be examined in 18 series of prostate biopsies obtained before and 1, 4, 7 and every 6 months after castration until recurrence in men with advanced CaP to identify genes that are up-regulated coincidental with the onset of recurrent proliferation.

- Characterize the expression of proliferation-associated genes identified in the CWR22 model in clinical specimens of 50 androgen-dependent and 25 androgen-independent CaPs using automated image analysis of immunohistochemical preparations of tissue microarrays (months 6-18)

The necessary antibodies have been obtained and optimal methods for immunostaining have been developed for 10 gene products of interest. The tissue microarrays are ready for immunostaining and analysis.

- Determine the time of onset of proliferation in the 18 sets of serial prostate biopsies performed before and after castration in men with advanced CaP using automated image analysis of Ki-67-stained tumor specimens (months 1-6)

The first 8 of the 16 invaluable sets of serial prostate biopsies obtained prior to and after castration for advanced prostate cancer have been sectioned and H&E stained. The slides are sub-optimal in terms of sectioning, staining quality and full face of tissue that compromises ability to make judgements about tumor morphology (and possibly if tumor is even present). We will use the Lineberger Tissue Core to embed future biopsies. 5 of 8 cases have cancer in the beginning couple and the end couple cores that show a reasonably similar morphology across all cores. The remaining 3 cases either have no cancer in all of the cores (2 cases) or only in the initial cores but not at the end (1 case) so no conclusions can be drawn about those. Androgen deprivation effects are seen to varying degrees in these cases. One of the cancer cases shows hyperchromatic and somewhat bizarre nuclei. Several of the cases show basal cell hyperplasia, squamous metaplasia and atrophy of benign glands. There is a possibility that tumor has been missed in some of the cases later in the time course of treatment because of the changes that androgen deprivation therapy produces in cancer causing it to be more easily missed in cores. These difficulties were discussed with Angelo DeMarzo, M.D., Ph.D. We will use racemase and p63 immunostaining to highlight the presence of malignant prostatic epithelial cells and basal cells in an attempt to enhance our ability to work with the serial prostate biopsies (Luo 2002; Rubin, 2002).

- Characterize the expression of the proliferation-associated genes that appear promising as initiators of recurrent cell proliferation after castration in preliminary study in the CWR22 model and the prostatectomy specimens in the 18 sets of serial prostate biopsies using automated image analysis of immunohistochemical preparations (months 6-18)

Awaiting progress on above work.

- Confirm the association of candidate genes with the onset of recurrent cell proliferation after castration using double staining to compare expression in proliferating (Ki-67 positive) versus non-proliferating (Ki-67 negative) cells in serial prostate biopsies that demonstrate the onset of androgen-independent growth (months 12-24)

Aim 3) Determine the effect of altering gene expression upon cell proliferation *in vitro* and serum PSA and tumor growth *in vivo*

Overview: The expression of candidate genes from Aim 2 will be manipulated *in vitro* using antisense probes and the effect upon cell proliferation measured using the androgen-sensitive LNCaP and LAPC-4 cell lines and CWR22 organ culture and the androgen-independent cell lines C4-2 (derived from LNCaP) and CWR-RCaP1 (derived from CWR22). Expression of individual genes will be inhibited *in vivo* to test for effects on tumor growth and serum PSA when antisense oligonucleotides are injected into groups of 12 mice bearing CWR22 tumors 110 days after castration. Effective treatments will be tested more rigorously in groups of 30 tumor-bearing mice.

- Obtain antisense oligonucleotides against best candidate genes from Aims 1 and 2 for use in cell lines and tumors (months 12-24)
- Determine the optimal dose and dosing interval for each antisense oligonucleotide and compare their effects upon cell proliferation using the androgen-sensitive LNCaP and LAPC-4 cell lines, CWR22 organ culture and androgen-independent cell lines C4-2 (derived from LNCaP) and CWR-R1 (derived from CWR22) (months 18-30)
- Determine the optimal dose and dosing interval of antisense oligonucleotides delivered by intraperitoneal injection and their effects on CWR22 tumor cell growth when delivered 110 days after castration (months 18-36)

We have not made any specific progress on Aim 3 since we don't have our gene targets identified yet. However, we have made progress that prepares for the use of oligos to address Aim 3. We demonstrated that antisense oligos can be used in prostate cancer cell lines and that they can be delivered in the nude mouse that constitutes the CWR22 model. Antisense was used *in vitro* to shift the splicing pattern of bcl-X between anti-apoptotic long and pro-apoptotic short forms in the human CaP cell line PC3 (Mercante, 2002b). bcl-X antisense was used to shift the splice site from the long to the short form that increased the sensitivity of PC3 cells to radiation and chemotherapy. This approach may have therapeutic implications since we demonstrated that the anti-apoptotic long form is over-expressed in CaP compared to benign prostate in frozen prostate tissues contained in our liquid nitrogen freezer.

The most often stated criticism of antisense therapy is inability to deliver antisense *in vivo*. We offer the following evidence to demonstrate that we can deliver antisense in our CWR22 nude mouse model. Ryzard Kole has developed a transgenic mouse model for functional assay of antisense activity using enhanced green fluorescent protein (EGFP). Similar to the bcl-X experiment using PC3 cells, a mutation was created that produces a splice variant that abrogates fluorescence (Sazani, 2002; Mercante, 2002a). This model was then used to determine whether antisense treatment would work *in vivo*. Antisense treatment restored fluorescence in the heart, kidney, liver and lung of the EGFP 654 nude mouse. The blood brain barrier blocked the antisense delivery and antisense did not reach the skin. This creates the possibilities that our CWR22 xenografts, which are implanted subcutaneously, may not receive antisense. This possibility is being examined currently in PC3 xenografts grafted into nude mice.

KEY RESEARCH ACCOMPLISHMENTS

- Identification of Nkx3.1, α -tubulin and IGFBP-5 as potential targets for preventing the development of CaP recurrence.
- Developed a hybrid immunostaining protocol for comparison of expression of antigens in proliferating versus non-proliferating cells.

REPORTABLE OUTCOMES

Manuscripts:

Mercatante DR, Mohler JL, Kole R. Cellular response to an antisense-mediated shift of bcl-x pre-mRNA splicing and antineoplastic agents. J Biol Chem 277: 49374-49382, 2002.

Kim D, Gregory CW, French FS, Smith GJ, Mohler JL: Androgen receptor expression and cellular proliferation during transition from androgen-dependent to recurrent growth after castration in the CWR22 prostate cancer xenograft. Am J Pathol 160:219-226, 2002.

Mohler JL, Morris TL, Ford OH III, Alvey RF, Sakamoto C, Gregory CW. Identification of differentially expressed genes associated with androgen-independent growth of prostate cancer. Prostate 51:247-255, 2002.

Tissue repository:

BrdU-labeled CWR22 tumor repository

Training supported by this award:

Mark A. Titus, PhD, post-doctoral fellow

CONCLUSIONS

We have made progress in the first year of this award to identify targets for antisense therapy that can be tested in *in vitro* in CaP cell lines and *in vivo* in the CWR22 model. The development of a hybrid immunostaining protocol for comparison of expression of antigens in proliferating versus non-proliferating cells has proven difficult. We next must modify our image analysis algorithms to allow quantitation. This effort will allow a more objective choice of gene target for *in vitro* and *in vivo* studies and should prove worthwhile the delay in meeting our

statement of work. The serial prostate biopsies have proven less informative than we desire but should still prove invaluable in the proposed studies.

REFERENCES

Fu H, Subramanian RR, Masters SC. 14-3-3 proteins: Structure, function, and regulation. *Ann Rev Pharmacol Toxicol* 40: 617-647, 2000.

Gregory CW, Johnson RT, Presnell SC, Mohler JL, French FS. Androgen receptor regulation of G1 cyclin and cyclin dependent kinase function in the CWR22 human prostate cancer xenograft. *J Andrology* 22:537-548, 2001.

Kim D, Gregory CW, Smith GJ, Mohler JL. Immunohistochemical quantitation of androgen receptor expression using color video image analysis. *Cytometry* 35:2-10, 1999.

Kim D, Gregory CW, French FS, Smith GJ, Mohler JL. Androgen receptor expression and cellular proliferation during transition from androgen-dependent to recurrent growth after castration in the CWR22 prostate cancer xenograft. *Am J Pathol* 160:219-226, 2002.

Luo J, Zha S, Gage WR, Dunn TA, Hicks JL, Bennett CJ, Ewing CM, Platz EA, Ferdinandusse S, Wanders RJ, Trent JM, Isaacs WB, De Marzo AM. Alpha-methylacyl-CoA racemase: a new molecular marker for prostate cancer. *Cancer Res* 62:2220-6, 2002.

Mercatante DR, Kole R. Control of alternative splicing by antisense oligonucleotides as a potential chemotherapy: effects on gene expression. *Bioch. Bioph. Acta* 1587: 126-132, 2002 [a].

Mercatante DR, Mohler JL, Kole R. Cellular response to an antisense-mediated shift of bcl-x pre-mRNA splicing and antineoplastic agents. *J Biol Chem* 277: 49374-49382, 2002 [b].

Mohler JL, Morris TL, Ford OH III, Alvey RF, Sakamoto C, Gregory CW. Identification of differentially expressed genes associated with androgen-independent growth of prostate cancer. *Prostate* 51:247-255, 2002.

Rubin MA, Zhou M, Dhanasekaran SM, Varambally S, Barrette TR, Sanda MG, Pienta KJ, Ghosh D, Chinnaiyan AM. Alpha-methylacyl coenzyme A racemase as a tissue biomarker for prostate cancer. *JAMA* 287:1662-1670, 2002.

Sazani P, Gemignani F, Kang S-H, Maier MM, Manoharan M, Persmark M, Bortner D, Kole R. Functional analysis of modified oligonucleotides in vivo. Systemic delivery, biodistribution and antisense effects. *Nature Biotech* 20:1228-1233, 2002.

Wainstein MA, He F, Robinson D, Kung H-J, Schwartz S, Giaconia JM, Edgehouse NL, Pretlow TP, Bodner DR, Kursh ED, Resnick MI, Seftel A, Pretlow TG. CWR22: androgen-dependent

xenograft model derived from a primary human prostatic carcinoma. *Cancer Res* 54:6049-6052, 1994.

Wakui H, Wright APH, Gustafsson J-A, Zilliacus J. Interaction of the ligand-activated glucocorticoid receptor with the 14-3-3 η protein. *J Biol Chem* 272: 8153-8156, 1997.

APPENDICES

Mercatante DR, Mohler JL, Kole R. Cellular response to an antisense-mediated shift of bcl-x pre-mRNA splicing and antineoplastic agents. *J Biol Chem* 277: 49374-49382, 2002.

Kim D, Gregory CW, French FS, Smith GJ, Mohler JL: Androgen receptor expression and cellular proliferation during transition from androgen-dependent to recurrent growth after castration in the CWR22 prostate cancer xenograft. *Am J Pathol* 160:219-226, 2002.

Mohler JL, Morris TL, Ford OH III, Alvey RF, Sakamoto C, Gregory CW. Identification of differentially expressed genes associated with androgen-independent growth of prostate cancer. *Prostate* 51:247-255, 2002.

Cellular Response to an Antisense-mediated Shift of Bcl-x Pre-mRNA Splicing and Antineoplastic Agents*

Received for publication, September 9, 2002, and in revised form, October 8, 2002
Published, JBC Papers in Press, October 14, 2002, DOI 10.1074/jbc.M209236200

Danielle R. Mercatante[‡], James L. Mohler[§], and Ryszard Kole^{‡¶}

From the [‡]UNC Lineberger Comprehensive Cancer Center and Departments of Pharmacology, [§]Surgery (Division of Urology), and Pathology and Laboratory Medicine, University of North Carolina, Chapel Hill, North Carolina 27599

Overexpression of Bcl-xL, an anti-apoptotic member of the Bcl-2 family, negatively correlates with the sensitivity of various cancers to chemotherapeutic agents. We show here that high levels of expression of Bcl-xL promoted apoptosis of cells treated with an antisense oligonucleotide (5'Bcl-x AS) that shifts the splicing pattern of Bcl-x pre-mRNA from the anti-apoptotic variant, Bcl-xL, to the pro-apoptotic variant, Bcl-xS. This surprising finding illustrates the advantage of antisense-induced modulation of alternative splicing *versus* down-regulation of targeted genes. It also suggests a specificity of the oligonucleotide effects since non-cancerous cells with low levels of Bcl-xL should resist the treatment. 5'Bcl-x AS sensitized cells to several antineoplastic agents and radiation and was effective in promoting apoptosis of MCF-7/ADR cells, a breast cancer cell line resistant to doxorubicin via overexpression of the *mdr1* gene. Efficacy of 5'Bcl-x AS combined with chemotherapeutic agents in the PC3 prostate cancer cell line may be translated to clinical prostate cancer since recurrent prostate cancer tissue samples expressed higher levels of Bcl-xL than benign prostate tissue. Treatment with 5'Bcl-x AS may enhance the efficacy of standard anti-cancer regimens and should be explored, especially in recurrent prostate cancer.

Cancers not completely eradicated by surgery or radiation (localized therapy) may escape control by chemotherapy (systemic therapy) because some cancer cells, especially those resistant to apoptosis, survive treatment (1, 2). For example, prostate cancer that recurs after potentially curative therapy, or that presents in an advanced stage, is palliated with androgen-deprivation therapy. Within several years most recur as androgen-independent, metastatic disease that leads to death. Recently, chemotherapy regimens have been developed that allow palliation in most patients. While such treatments may lead to re-remissions of 1 year or more, they have not proven to increase survival (3–5).

Chemotherapeutic resistance usually arises due to overexpression of anti-apoptotic proteins such as Bcl-2 and Bcl-xL (2, 6–8). Bcl-2 is regarded as one of the most important proteins protecting cancer cells from apoptosis and, to date, may be the

most highly studied member of the Bcl-2 family. However, in an examination of 60 different cell lines from the National Cancer Institute, Bcl-xL was shown to provide equivalent or greater protection against cytotoxic agents than Bcl-2. Higher levels of Bcl-xL correlated with decreased cellular sensitivity toward a variety of chemotherapeutic reagents; there was no such correlation for Bcl-2 (6). Other studies have shown that high levels of Bcl-xL contributed to increased risk of metastasis in breast cancer (9) and protected cancer cells from chemotherapeutic agents (10, 11). In addition, cancer cells were sensitized to various apoptosis-inducing agents if Bcl-xL levels were decreased (12, 13).

Bcl-xL and Bcl-xS are splice variants produced by alternative splicing of Bcl-x pre-mRNA (14). While Bcl-xL is anti-apoptotic, Bcl-xS has been shown to induce cell death (15, 16) and sensitize cancer cells to chemotherapeutic agents (17–20). Bcl-xS inhibits the anti-apoptotic effects of Bcl-xL and Bcl-2, possibly by forming heteroduplexes with these proteins (21) and/or by acting as a dominant negative gene product (22). Decreasing Bcl-xL and increasing Bcl-xS levels may initiate pro-apoptotic events through various cellular mechanisms that, alone or in synergy with the action of antineoplastic agents, lead to cell death.

We have shown previously that a 2'-O-methyl-oligoribonucleoside phosphorothioate (5'Bcl-x AS)¹ targeted to the downstream alternative 5'-splice site in exon 2 of Bcl-x pre-mRNA shifted splicing from the Bcl-xL to Bcl-xS splice variants; this treatment decreased the levels of Bcl-xL and increased the levels of Bcl-xS proteins (23). The shift in splicing induced cell death in oligonucleotide-treated PC3 prostate cancer cells and to a lesser extent in MCF-7 breast cancer cells. In A549 lung epithelial cells, a similar treatment alone was ineffective; cell death resulted only from co-administration of radiation or cisplatin (24). These findings prompted us to investigate the differences in cellular responses as a result of oligonucleotide-induced modification of Bcl-x pre-mRNA splicing. We found that the endogenous level of Bcl-x is the main factor that determines the extent of cell death induced by 5'Bcl-x AS. Treatment of PC3 and MCF-7 cells (two cell lines that express different levels of Bcl-xL) with 5'Bcl-x AS sensitized both cell lines to various chemotherapeutic agents and radiation and increased cell death at lower doses of these agents. Finally, prostate cancer expressed higher levels of Bcl-xL protein than benign prostate. These results suggest that

* This work was supported in part by Grants PO1-GM59299-01 (to R. K.) and PO1-CA77739 (to J. L. M.) from the National Institutes of Health. The costs of publication of this article were defrayed in part by the payment of page charges. This article must therefore be hereby marked "advertisement" in accordance with 18 U.S.C. Section 1734 solely to indicate this fact.

¶ To whom correspondence should be addressed: University of North Carolina, UNC-Lineberger Comprehensive Cancer Center, CB7295, Chapel Hill, NC 27599-7295. Tel.: 919-966-1143; Fax: 919-966-3015; E-mail: kole@med.unc.edu.

¹ The abbreviations used are: 5'Bcl-x AS, antisense oligonucleotide targeted to the downstream alternative 5'-splice site of Bcl-x pre-mRNA; 5-FdU, 5-fluorodeoxyuridine; 5-FU, 5-fluorouracil; ASO, antisense oligonucleotide; FCS, fetal calf serum; ER, estrogen receptor; RPA, RNase protection assay; RT, reverse transcription; Gy, Gray; GAPDH, glyceraldehyde-3-phosphate dehydrogenase; MEM, modified essential medium.

5'Bcl-x AS treatment may augment the effectiveness of radiation and chemotherapy for prostate cancer.

EXPERIMENTAL PROCEDURES

Cells Lines and Prostate Tissue Samples—The treated human cancer cell lines were from prostate (PC3, DU145), breast (MCF-7, MDA-MB-231, BT-549, Hs578T) and cervical (HeLa) cancers. They included four p53 mutant cells (PC3, DU145, MDA-MB-231, Hs578T) (25–28) and three p53-positive cells (MCF-7, BT549, HeLa) (25, 28–30). Among the breast cancer cell lines, two were ER-negative (MDA-MB-231, Hs578T) (28) and two were ER-positive (MCF-7, BT549) (28, 29). PC3 and DU145 were androgen-insensitive prostate cancer cell lines. All cell lines were originally from the ATCC and grown in a humidified incubator with 5% CO₂ at 37 °C. All cells were cultured in the presence of penicillin/streptomycin or, for HeLa cells gentamycin/kanamycin, in the following media. PC3: DMEM/F12 (Dulbecco's Modified Eagle's Medium), 10% fetal calf serum (FCS); MCF-7: MEM (modified essential medium), 10% FCS, 1× sodium pyruvate (Invitrogen), 1× non-essential amino acids (Sigma), 10 µg/ml insulin (Invitrogen); MDA-MB 231 and Hs578T: Dulbecco's modified Eagle's medium, 10% FCS, insulin (10 µg/ml); BT 549: RPMI 1640 (Invitrogen), 10% FCS, insulin (1 µg/ml); HeLa: MEM, 5% FCS, 5% horse serum, L-glutamine (2 mM; Invitrogen); and DU145: MEM, 10% FCS, 1× sodium pyruvate, 1× non-essential amino acids. Twenty-four hours prior to oligonucleotide treatment, all cells were plated in 1 ml of media in 24-well plates at a density of 7×10^4 per well.

Research specimens were recovered from prostate tissue stored in liquid nitrogen. Androgen-independent prostate cancer had been obtained by transurethral resection from 10 men who presented with urinary retention from recurrent prostate cancer 7–92 months after androgen deprivation therapy. Histologic examination revealed poorly differentiated prostate cancer (Gleason scores 8–10) that represented an average of 92% (ranged from 72–99%) of the cross-sectional area of the tissue sections. Ten specimens of benign prostate tissue had been obtained from portions of adenoma removed at open prostatectomy; absence of cancer was confirmed by frozen section.

Oligonucleotide Treatment—2'-O-methyl-oligoribonucleoside phosphorothioate 18-mer, antisense to the 5'-splice site of Bcl-xL (AC-CCAGCCGCCGUUCUCC; 5'Bcl-x AS) was synthesized by Trilink Biotechnologies, Inc. (San Diego, CA). 2'-O-methyl oligoribonucleoside phosphorothioate 18-mers with randomized sequence and/or antisense to human β -globin IVS2–705 sequence (31) were used as negative controls; they were synthesized by Hybridon, Inc (Cambridge, MA). Cells were treated with oligonucleotides complexed with DMRIE-C (8 µg/ml, Invitrogen) cationic lipid delivery agent (23).

Treatment with Antineoplastic Agents and Radiation—Cisplatin, 5-FU (5-fluorouracil), 5-FdU (5-fluorodeoxyuridine), etoposide, and doxorubicin were obtained from Sigma. Their concentrations used in treatment of oligonucleotide-treated PC3 and MCF-7 cells were in the ranges of 0.001–10 µg/ml for cisplatin and 0.001–10 µM for the remaining four drugs. 48 h after oligonucleotide transfection, the cells were treated with the above compounds for the times indicated in the text and figure legends. The variations in treatment were designed to maximize the response in subsequent assays (see below).

In radiation experiments, cells were replated in 10-cm plates 24 h after oligonucleotide treatment. After overnight culture, cells were irradiated using a ⁶⁰Co γ -irradiator at doses indicated in Fig. 7. The numbers of re-plated and irradiated cells were: control PC3 cells, 500 at 0–2 Gy, 1000 at 4 Gy; 5'Bcl-x AS-transfected PC3 cells: 500 at 0 Gy, 1000 at 1 and 2 Gy, 2000 at 4 Gy; control MCF-7 cells, 1000 at 0–2 Gy, 2000 at 4 Gy; 5'Bcl-x AS-transfected MCF-7 cells: 1000 at 0 Gy, 2000 at 1 and 2 Gy, 4000 at 4 Gy. After irradiation, cells were cultured, and colonies stained and counted on day 10 of culture (see below), and the percent viability (or replating efficiencies) was calculated.

RNA Isolation and Reverse Transcription-PCR (RT-PCR)—These procedures were carried out as previously described (23). Briefly, 48 h after oligonucleotide transfection, cells were lysed in 1 ml of TRI-reagent (MRC, Cincinnati, OH), and total RNA was isolated. RT-PCR was performed with rTth DNA polymerase (PerkinElmer Life Sciences, Branchburg, NJ) in the presence of 0.2 µCi of [³²P]dATP and forward (CATGGCAGCACTAAAGCAAG) and reverse primers (GCATTGTTC-CCATAGAGTTCC) at 70 °C, 15 min for the RT step followed by PCR: 95 °C, 3 min, 1 cycle; 22 cycles of 95 °C for 30 s, 56 °C for 30 s, 72 °C for 1 min; and final extension at 72 °C for 7 min.

Colony Formation Assay—48 h after oligonucleotide treatment, 500 cells for PC3, DU145, MDA-MB 231, BT 549, MCF-7/ADR, and HeLa and 1000 cells for MCF-7 and Hs578T were re-plated in 10-cm plates. After 10 days under normal culture conditions surviving colonies were

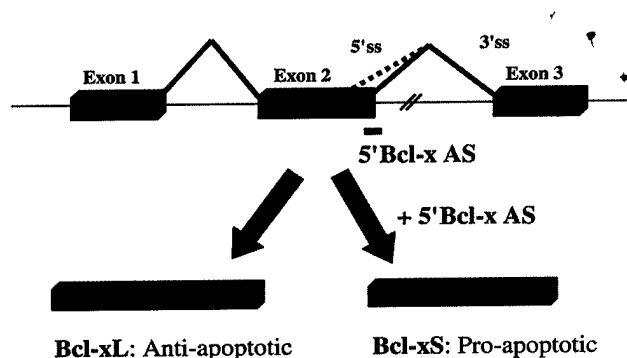


FIG. 1. **Alternative splicing of Bcl-x pre-mRNA.** Use of the upstream alternative 5'-splice site (dotted line) in exon 2 yields the shorter, pro-apoptotic splice variant, Bcl-xS. Use of the downstream 5'-splice site (thick solid line) results in the longer, anti-apoptotic splice variant, Bcl-xL. Short bar below this splice site indicates 5'Bcl-x AS, an antisense 2'-O-methyl phosphorothioate oligonucleotide, designed to shift the splicing pattern from Bcl-xL to Bcl-xS. Boxes, exons; thin lines, introns.

stained with 5% methylene blue (Sigma) in 50% ethanol for 10 min. Colonies larger than 50 cells were counted. For chemotherapeutic dose-response experiments, re-plated, oligonucleotide-treated cells were treated for 24 h with the chemotherapeutic agents. After treatment with chemotherapeutic agents, the cells were washed with HBSS (Hank's Buffered Saline Solution, Invitrogen), and fresh medium was added. The remainder of the procedure was the same.

Bcl-xL Western Blot—Total protein was prepared by lysing cells (one well of a 24-well plate) or lysing prostate tumor tissues (200 mg tissue sections finely ground to a powder) in radioimmune precipitation assay (RIPA) buffer (50 mM Tris-HCl, 150 mM NaCl, 5 mM EDTA, 1% Triton X-100, 0.1% SDS, 1% sodium deoxycholate), and a mixture of protease inhibitors (15 µl for every 1 ml of RIPA buffer, Sigma). 20 µg of total protein were electrophoresed on a 15% SDS-polyacrylamide gel and electrotransferred to polyvinylidene difluoride membranes. Blots were probed with Bcl-xL (1:1000 dilution; Transduction Laboratories, Lexington, KY) followed by a horseradish peroxidase (HRP)-conjugated secondary antibody (1:5000 dilution; Bio-Rad). Bcl-xL migrated at ~30 kDa. Equal loading and transfer were confirmed by staining the membranes with Ponceau S (Sigma) and blotting with β -tubulin antibody (1:4000 dilution; Sigma) followed by an HRP-conjugated secondary antibody (1:5000 dilution; Sigma); β -tubulin protein migrated at ~55 kDa. Protein was visualized with ECL Plus (Amersham Biosciences) treatment.

RNAse Protection Assay (RPA)—Untreated cells were analyzed for levels of Bcl-xL, Bcl-xS, Bax, Bak, Bcl-2, Mcl-1, and GAPDH genes with a multiprobe template set (hAPO-2; BD Pharmingen, San Diego, CA) and RPA II RNase protection assay kit (Ambion, Inc., Austin, TX). Reactions were carried out according to the manufacturers' protocols.

Statistical Analysis—Prism (Graph Pad) software was used to generate dose response curves, calculate LC₅₀ values, and for other statistical analyses indicated in the figure and table legends.

RESULTS

Cell Death Affected by a Shift in Splicing from Bcl-xL to Bcl-xS—To shift the alternative splicing pathway of Bcl-x pre-mRNA from Bcl-xL to Bcl-xS, seven different cell lines were treated with 5'Bcl-x AS antisense oligonucleotide targeted to the downstream alternative 5'-splice site of exon 2 (Fig. 1) and delivered to the cells with the aid of DMRIE-C cationic lipid reagent. The treated cell lines originated from prostate (PC3, DU145), breast (MCF-7, MDA-MB-231, BT-549, Hs578T), and cervical (HeLa) cancers and represented distinct genetic backgrounds (see "Experimental Procedures").

RT-PCR analysis of total RNA from untreated cells showed that in all cell lines Bcl-xL mRNA was essentially the only expressed splice variant; Bcl-xS was barely or not at all detectable (Fig. 2A, lane 1). Since the uptake of the lipid-oligonucleotide complex or the oligonucleotide antisense activity may vary in different cells, for each cell line, the oligonucleotide concentration was adjusted such that the splicing was shifted

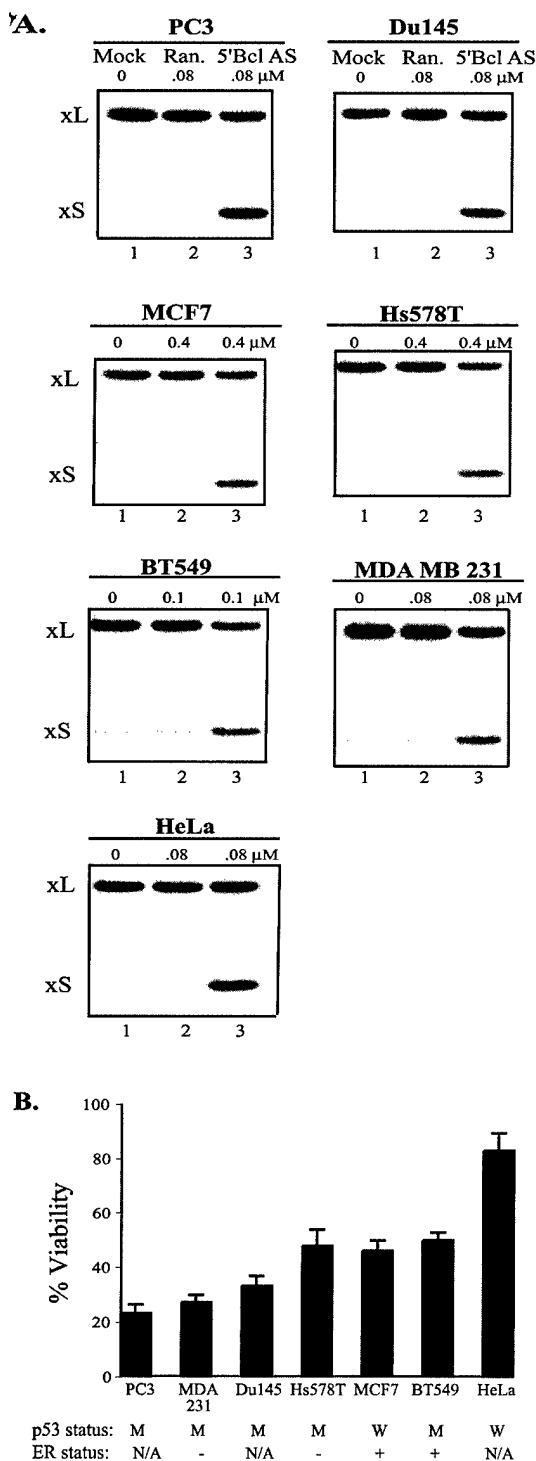


FIG. 2. Cellular response to 5'Bcl-x AS treatment. A, shift in Bcl-xL/xS splice variant ratio. RT-PCR analysis of total RNA from 5'Bcl-x AS-treated cells (see text and "Experimental Methods"). The cell lines (prostate cancer, DU145 and PC3; breast cancer, MCF-7, Hs578T, BT-549, MDA-MB-231; cervical cancer, HeLa) are indicated above the panels. Lane 1, mock transfection; lane 2, transfection with randomized oligonucleotide; lane 3, transfection with 5'Bcl-x AS. The concentrations of the oligonucleotides are indicated (top). B, 5'Bcl-x AS-induced death of treated cell. Cells treated with the concentrations of 5'Bcl-x AS that elicited 50% shift in Bcl-xL/xS splicing in each cell line were tested in a clonogenic assay ("Experimental Methods"). Cell viability is expressed as percent colonies formed 10 days after treatment and normalized versus control cells treated with the same concentration of randomized oligonucleotide. In this and subsequent figures error bars represent the S.D. from at least three independent experiments. Mutant (M) and wild type (W) p53 and ER status are indicated below the graph.

~50–60%. Note that RT-PCR was carried out with 32 P-labeled dATP, which is incorporated into Bcl-xL and -xS spliced products with a 1.2:1 ratio. Thus, the autoradiograms shown in Fig. 2A slightly underrepresent the amount of newly generated Bcl-xS mRNA. The extent of the oligonucleotide-induced shift in splicing was confirmed by RPA (data not shown).

The effects of the treatment with 5'Bcl-x AS on the survival of the cells from all seven cell lines was determined by a colony formation assay. This method was chosen because it quantifies the cumulative cell death over a prolonged 10-day period of time. Short term apoptosis assays were not appropriate since the time course of apoptosis induction varies from cell line to cell line making it difficult to compare the overall extent of apoptosis among different cell lines. The results shown in Fig. 2B demonstrated that the oligonucleotide treatment led to death of the cells from all cell lines; PC3 cells were the most, and HeLa cells were the least susceptible.

Endogenous Levels of Bcl-xL Determine the Cellular Response to 5'Bcl-x AS—Since the extent of Bcl-xL/xS splicing modification was normalized to approximately the same 50–60% level (Fig. 2A) it appeared that other factors must have contributed to the variability of the cellular response to 5'Bcl-x AS treatment. No clear correlation was found between susceptibility to 5'Bcl-x AS treatment and the level of expression of functional p53 or ER genes; this indicated that Bcl-xL/Bcl-xS effects are p53 (32, 33) and ER-independent (Fig. 2B). Furthermore, there was no correlation between 5'Bcl-x AS susceptibility, and the levels of expression of several Bcl-2 family members (Bak, Mcl-1, Bcl-2, and Bax) determined by RPA of total RNA from the seven cell lines (Fig. 3).

To further address this issue, an examination of the levels of Bcl-xL mRNA was carried out by RPA. The results showed that the levels of Bcl-xL were highest in PC3 cells, followed by MDA 231, DU145, Hs578T, MCF-7, BT549 and lowest in HeLa cells (Fig. 4, A and B). Analysis of Bcl-xL protein by immunoblotting with anti-Bcl-xL antibody established the same rank order of Bcl-xL expression levels (Fig. 4, C and D). There was a high degree of correlation (p value of < 0.0001 and $r^2 = 0.9601$, by Pearson correlation) between the levels of Bcl-xL protein in untreated cell lines and death of 5'Bcl-x AS-treated cells, indicating that cells containing higher levels of Bcl-xL were more susceptible to 5'Bcl-x AS oligonucleotide treatment.

This counterintuitive result, that increased expression of anti-apoptotic Bcl-xL at the same time facilitates cell death of 5'Bcl-x AS-treated cells, is best explained by the data illustrated in Fig. 5, A and B. The seven different cell lines were treated with 5'Bcl-x AS at concentrations indicated in Fig. 2A that resulted in 50–60% shift in Bcl-x pre-mRNA splicing. Despite the fact that the relative amounts of Bcl-xL/xS mRNAs were the same in all cell lines (*i.e.* the ratio of Bcl-xL to -xS was ~50–60%), RPAs of total RNA with a Bcl-xS-specific probe showed that the absolute levels of Bcl-xS mRNA varied substantially (Fig. 5). PC3 cells had the highest and HeLa cells the lowest content of this RNA, consistent with the expression levels of Bcl-xL and not the extent of the shift in splicing. These data suggest that highly expressing cells such as PC3 cells have high levels of Bcl-x pre-mRNA, which when spliced produced large amounts of Bcl-xL mRNA. When targeted with 5'Bcl-x AS oligonucleotide splicing of Bcl-x pre-mRNA resulted in large amounts of Bcl-xS mRNA (Fig. 5) and presumably Bcl-xS protein. Previously observed differences in the level of Bcl-xS protein in oligonucleotide-treated PC3 and MCF-7 cells support this conclusion (23).

5'Bcl-x AS Sensitizes MCF-7 and PC3 Cells to Antineoplastic Treatments—The 5'Bcl-x AS-induced shift in splicing may be less effective against cancers with low Bcl-x expression levels

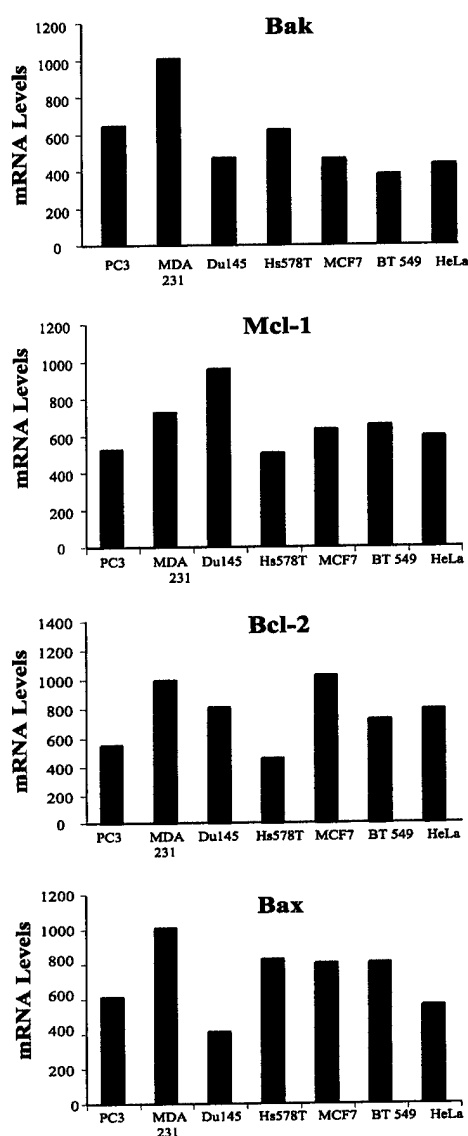


FIG. 3. Relative levels of expression of anti-apoptotic genes. Ribonuclease protection assays (see "Experimental Methods") for Bak, Mcl-1, Bcl-2, and Bax (indicated above the graphs) were carried out on total RNA from the cell lines indicated below the graphs. The mRNA levels are normalized to the levels of GAPDH mRNA and expressed in arbitrary units from NIH Image. Results are an average from two samples.

(see also "Discussion" for additional considerations). Thus, we sought to determine if the applicability of this approach could be extended to more resistant cells if the 5'Bcl-x AS treatment is combined with conventional antineoplastic agents. The experiments were carried out on the MCF-7 breast cancer cell line, a cell line relatively resistant to oligonucleotide treatment, and the oligonucleotide-susceptible PC3 prostate cancer cell line. Five apoptosis-inducing agents, cisplatin, doxorubicin, 5-FU, 5-FdU, and etoposide, which exert their cytotoxic effects through different mechanisms (see "Discussion") were selected for these experiments. All of these chemotherapeutic agents are a part of the standard set of anticancer agents included in the National Cancer Institute's drug screen (6).

Dose response curves were generated for MCF-7 cells treated with 0.1 and 0.4 μ M 5'Bcl-x AS followed by chemotherapeutic agents. 0.4 μ M random oligonucleotide-transfected or mock-transfected cells served as negative controls. 0.1 and 0.4 μ M 5'Bcl-x AS alone resulted in ~35 and 50% shift in splicing and

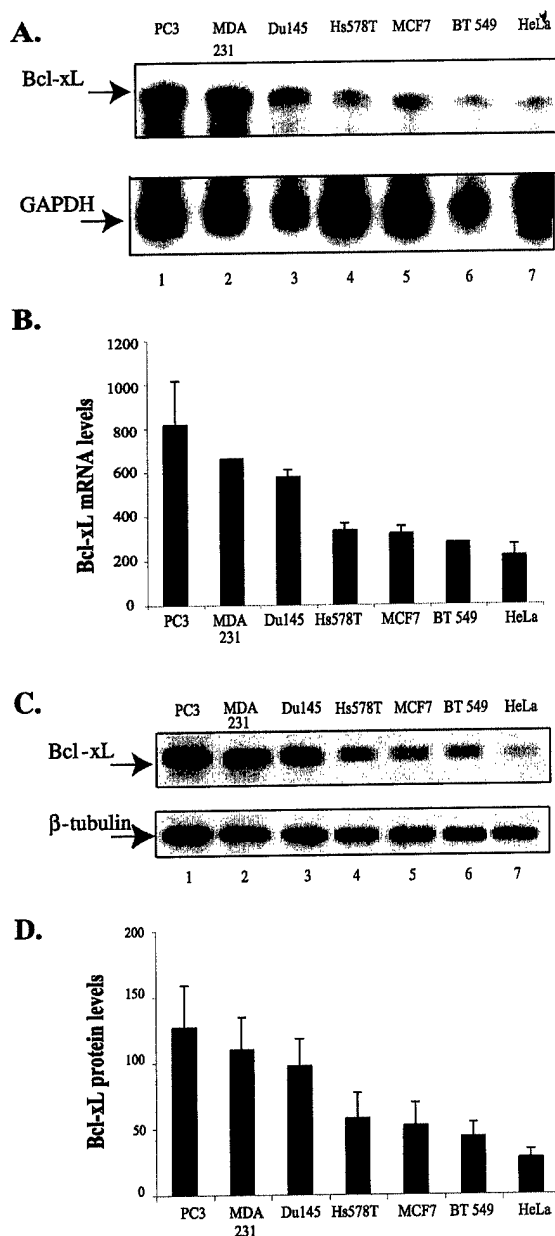


FIG. 4. Variability of Bcl-xL mRNA and protein levels. A, representative gel analysis of RNA protection assay for Bcl-xL (upper panel) and GAPDH (lower panel) mRNA levels. B, relative Bcl-xL mRNA levels, normalized for GAPDH, and expressed in arbitrary units from NIH Image. C, representative immunoblot analysis of Bcl-xL and β -tubulin protein levels (upper and lower panels, respectively). D, relative levels of Bcl-xL protein, normalized for β -tubulin, and expressed in arbitrary units from NIH Image.

59 and 38% viability, respectively (data not shown). The latter values were normalized to 100% in order to determine the LC_{50} of the different drugs (see "Experimental Methods"). Examples of the experimental data for cisplatin and doxorubicin are illustrated in Fig. 6, A and B. The summary of the data for all the drugs and MCF-7 and PC3 cells is in Tables I and II.

For MCF-7 cells, the 0.4 μ M concentration of 5'Bcl-x AS markedly decreased the LC_{50} values for cisplatin (>5-fold) and doxorubicin (>6-fold) (Table I). Although the oligonucleotide also sensitized the cells to a statistically significant degree to 5-FdU, the effect was not dose-dependent (see "Discussion"); the effect was even lower for etoposide. The shift in Bcl-x pre-mRNA splicing did not alter the sensitivity of MCF-7 cells to 5-FU. Treatment of PC3 cells with 5'Bcl-x AS at concentra-

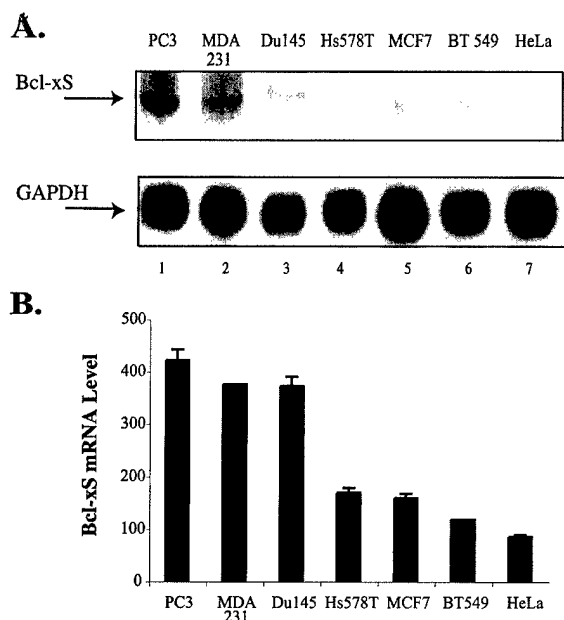


FIG. 5. Levels of Bcl-xS mRNA in 5'Bcl-x AS-treated cells. *A*, representative gel analysis of RNA protection assay for Bcl-xS (upper panel) and GAPDH (lower panel) mRNA levels in 5'Bcl-x AS (concentrations were as indicated in the legend to Fig. 2)-treated cells. *B*, relative Bcl-xS mRNA levels, normalized for GAPDH, and expressed in arbitrary units from NIH Image.

tions of 0.01 and 0.08 μM led to a 35 and 55% shift in Bcl-x pre-mRNA splicing and, respectively, to 58 and 25% viability (data not shown). Addition of cisplatin and 5-FdU to oligonucleotide-treated (0.08 μM 5'Bcl-x AS) PC3 cells led to a 10-fold decrease in LC_{50} of these drugs. The LC_{50} values of etoposide, 5-FU, and doxorubicin were 2–3-fold lower in 5'Bcl-x AS (0.08 μM)-treated PC3 cells than that in control cells. For the latter three drugs, oligonucleotide dose dependence was not found.

The effects of the oligonucleotide and antineoplastic treatments on cell viability in all the experiments were assayed in long term colony formation assays in tissue culture plates. Thus, it could be argued that there is no evidence that these treatments led to cell death by increasing apoptosis. We have shown previously that the shift in Bcl-xL/xS splicing induced apoptosis in PC3 and MCF-7 cells (23). We confirmed that the combination of 5'Bcl-x AS with cisplatin or 5-FdU for PC3 cells and with doxorubicin for MCF-7 cells induced PARP cleavage (poly(ADP)-ribose polymerase, an indicator of apoptosis) to a greater extent than each agent alone, as expected (data not shown).

Soft agar colony formation tests were carried out to confirm that the oligonucleotide/drug treatments caused cell death and not merely reduced the ability of the treated cells to attach to the culture plate. The 5'Bcl-x AS-transfected PC3 and MCF-7 cells were treated with cisplatin, doxorubicin, 5-FU, 5-FdU, and etoposide at the LC_{50} concentrations of these drugs shown in Tables I and II. Colony formation in soft agar and the calculated effects of the treatments on cell viability closely mirrored those obtained in the plate-based clonogenic assay (data not shown). Thus, the combined results of the PARP and soft agar assays indicate that the above treatments increased apoptotic cell death.

5'Bcl-x AS Sensitizes MCF-7 and PC3 Cells to Radiation—Overexpression of Bcl-xL is an important factor in mediating radioresistance (34) whereas cells with lower levels of Bcl-xL are more sensitive to radiation-induced apoptosis (35). Furthermore, it was found that radiation down-regulates Bcl-xL in

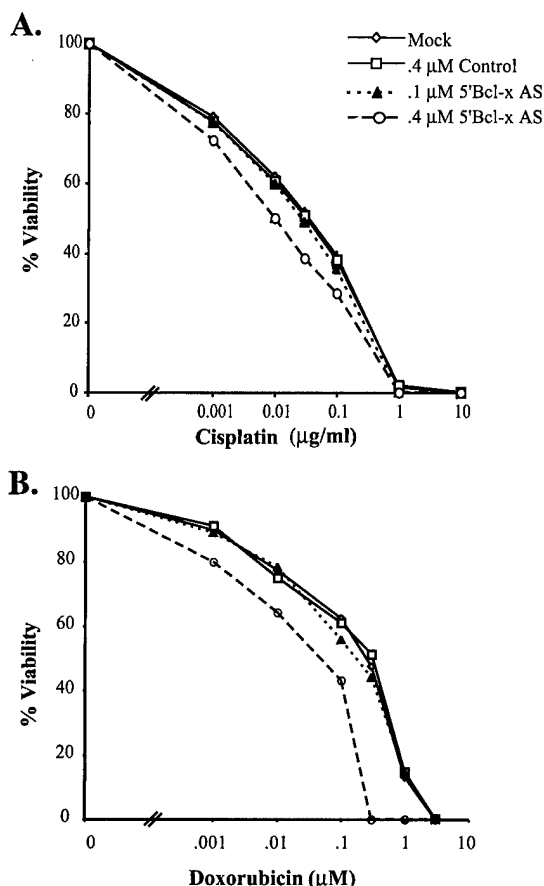


FIG. 6. Sensitization of MCF-7 cells to cisplatin and doxorubicin by 5'Bcl-x AS. *A* and *B*, dose response curves to cisplatin and doxorubicin of 5'Bcl-x AS-treated cells. The clonogenic assays were performed on MCF-7 cells transfected with the oligonucleotides at concentrations indicated in the panel followed by treatment with increasing concentrations of the drug. Cell viability of drug-treated cells is expressed as percent of colonies formed after treatment and normalized versus control cells treated with the oligonucleotide only. These data were used to calculate drug LC_{50} values. See "Experimental Procedures" for more details.

MCF-7 cells (36). Thus, it seemed likely that the oligonucleotide-induced shift in Bcl-xL/Bcl-xS splicing would sensitize cancer cells to radiation-induced apoptosis. Transfection of MCF-7 and PC3 cells with 5'Bcl-x AS (0.1 and 0.4 μM for MCF-7 and 0.01 and 0.08 μM for PC3 cells), followed by exposure to 1–4 Gy doses of radiation, resulted in a statistically significant reduction of cell viability (Fig. 7, *A* and *B*). At 2 Gy and 0.4 μM 5'Bcl-x AS oligonucleotide, MCF-7 cell viability was reduced to 24%, compared with 40% for control oligonucleotide-transfected cells. At the highest dose (4 Gy) the viability was further reduced in a dose-dependent fashion to 5.8 and 3.4% for 0.1 and 0.4 μM Bcl-x AS, respectively, compared with 14.5% for control oligonucleotide-transfected cells.

PC3 cells were found to be more sensitive to the combined oligonucleotide-radiation treatment. Cell viability was reduced close to 2-fold even at low doses (0.01 μM oligonucleotide and 1 Gy radiation). Under these conditions viability of the cells was lower than that of control cells irradiated at a 2-Gy dose (Fig. 7*B*). As the radiation dose increased, the effects of the shift in Bcl-xL/Bcl-xS splicing became less pronounced; at 4 Gy there was no further sensitization, presumably because the radiation alone induced massive cell death.

5'Bcl-x AS Induces Cell Death in the Multidrug-resistant Cell Line, MCF-7/ADR—Since treatment of cancer cells with chemotherapeutic agents may select resistant cells, we sought to

TABLE I
 LC_{50} results for MCF7 cells transfected with 5'Bcl-x AS

MCF7 cells were transfected with 0.1 and 0.4 μ M 5'Bcl-x AS that yielded, respectively, a 35 and 55% shift in splicing from Bcl-xL to Bcl-xS, or with a control oligonucleotide. LC_{50} values were obtained from dose response curves, as shown in Fig. 6. See "Experimental Procedures" for more details. Results are the mean values from three independent experiments. S.D. for all values were equal to or less than 0.02.

Cell line	Treatment	Etoposide μ M	5-FU μ M	Cisplatin μ g/ml	5-FdU μ M	Doxorubicin μ M
MCF-7	Mock	0.94	1.4	0.063	5.5	0.26
	0.4 μ M Control	0.84	1.1	0.061	5.4	0.29
	0.1 μ M 5Bcl-x AS	0.48 ^a	1.0	0.056 ^a	1.8 ^a	0.19 ^a
	0.4 μ M 5Bcl-x AS	0.49 ^a	0.96	0.012 ^b	1.4 ^a	0.041 ^b
LC_{50} decrease (0.4 μ M 5'Bcl-x AS vs. Mock):		1.9	1.1 (NS)	5.3	3.9	6.3

^a Significant difference from control cells ($p < 0.05$; one way ANOVA with Tukey post-hoc test).

^b Significant difference from control and 0.1 μ M 5'Bcl-x AS-treated cells ($p < 0.05$; one way ANOVA with Tukey post-hoc test).

^c NS, Not significant.

TABLE II
 LC_{50} results for PC3 cells transfected with 5'Bcl-x AS

PC3 cells were transfected with concentrations of 5Bcl-x AS (0.01 and 0.08 μ M) that yielded, respectively, a 35 and 50% shift in splicing from Bcl-xL to Bcl-xS. S.D. for all values were equal to or less than 0.023. Other details are as in the legend to Table 1.

Cell line	Treatment	Etoposide μ M	5-FU μ M	Cisplatin μ g/ml	5-FdU μ M	Doxorubicin μ M
PC3	Mock	2.2	12.2	0.19	5.8	0.030
	0.08 μ M Control	2.1	13.0	0.15	4.9	0.029
	0.01 μ M 5BclAS	0.67 ^a	5.0 ^a	0.13 ^a	1.5 ^a	0.017 ^a
	0.08 μ M 5BclAS	0.62 ^a	3.7 ^b	0.02 ^b	0.56 ^b	0.016 ^a
LC_{50} decrease (0.08 μ M 5'Bcl-x AS vs. Mock):		3.5	3.3	9.5	10.4	1.9

^a Significant difference from control cells ($p < 0.05$; one-way ANOVA with Tukey post-hoc test).

^b Significant difference from control and 0.01 μ M 5'Bcl-x AS-treated cells ($p < 0.05$; one way ANOVA with Tukey post-hoc test).

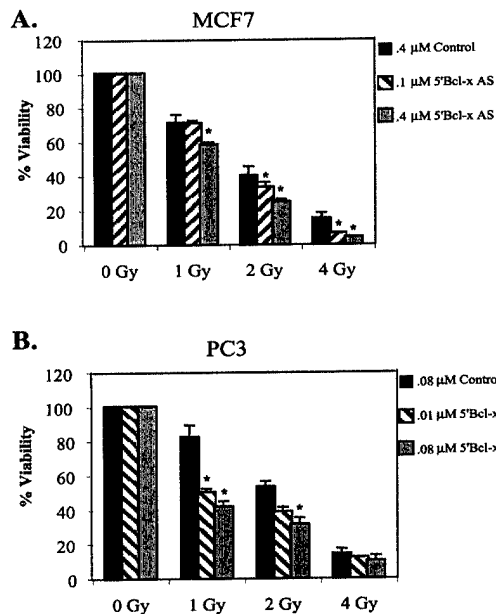


FIG. 7. Treatment with 5'Bcl-x AS sensitizes MCF-7 and PC3 cells to radiation. A, MCF-7 cells; B, PC3 cells. Clonogenic assay of cells transfected with the oligonucleotides at concentrations indicated in the figure followed by radiation at 1–4 Gy. Cell viability of irradiated cells is expressed as percent colonies formed after treatment and normalized versus control cells treated with the oligonucleotide only. Asterisk indicates statistically significant difference versus control cells ($p < 0.05$; one-way analysis of variance with Tukey post-hoc test).

determine if the oligonucleotide-induced shift in Bcl-xL/xS splicing caused apoptosis in chemotherapy-resistant cells. MCF-7/ADR cells, a p53 mutant (25) breast cancer cell line, are highly resistant to apoptosis induced by chemotherapeutic agents such as doxorubicin (37). Overexpression of the *mdr1* gene, which codes for P-glycoprotein, is the principal mecha-

nism of the chemoresistance for these cells (38–41). Treatment of MCF-7/ADR cells with 5'Bcl-x AS oligonucleotides resulted in a dose-dependent shift in splicing from Bcl-xL to Bcl-xS (Fig. 8A). The EC_{50} of 5'Bcl-x AS (0.08 μ M) was comparable to its EC_{50} in PC3 cells (0.08 μ M) and 5-fold lower than in parent MCF-7 cells (0.4 μ M). This effect appears to be due to increased uptake of the oligonucleotide-DMRIE-C complex into the nuclei (data not shown, see "Discussion"). The shift in splicing led to a dose-dependent decrease in the viability of the MCF-7/ADR cells (Fig. 8B). Although the 50% shift in Bcl-xL/xS splicing was achieved at a 5'Bcl-x AS concentration lower than that in MCF-7 cells, decreases in cell viability were comparable in the two cell lines (compare Figs. 2B and 8B).

In order to examine this observation in more detail, the level of Bcl-xL protein in MCF-7/ADR cells was determined and plotted versus cell viability and compared with the other cell lines studied. The level of Bcl-xL was similar to that of the parent MCF-7 cells (Fig. 8C). The decrease in cell viability was similar and agreed with the results obtained for other cell lines (Fig. 8C, $p < 0.0001$ and $r^2 = 0.9480$ by Pearson correlation). Thus, despite apparent changes in the oligonucleotide uptake resulting in increased sensitivity of Bcl-xL/xS splicing to oligonucleotide treatment, the decrease in cell viability remained unchanged suggesting that it depended only on the endogenous level of Bcl-x pre-mRNA as reflected in the levels of Bcl-xL protein.

High Expression of Bcl-xL in Prostate Cancer—Since the androgen-insensitive prostate cancer cell lines, PC3 and DU145, had among the highest levels of Bcl-xL, we tested if clinical specimens of prostate cancer recurrent after androgen deprivation therapy exhibited increased expression of this gene. Immunoblot analysis of prostate cancer and benign prostate samples showed significant differences in the levels of Bcl-xL between the two groups ($p = 0.0012$, 2-tailed Student's *t* test; Fig. 9). This suggests that Bcl-xL may play a role in the progression of prostate cancer and that modulation of its expression may be a means of controlling that progression.

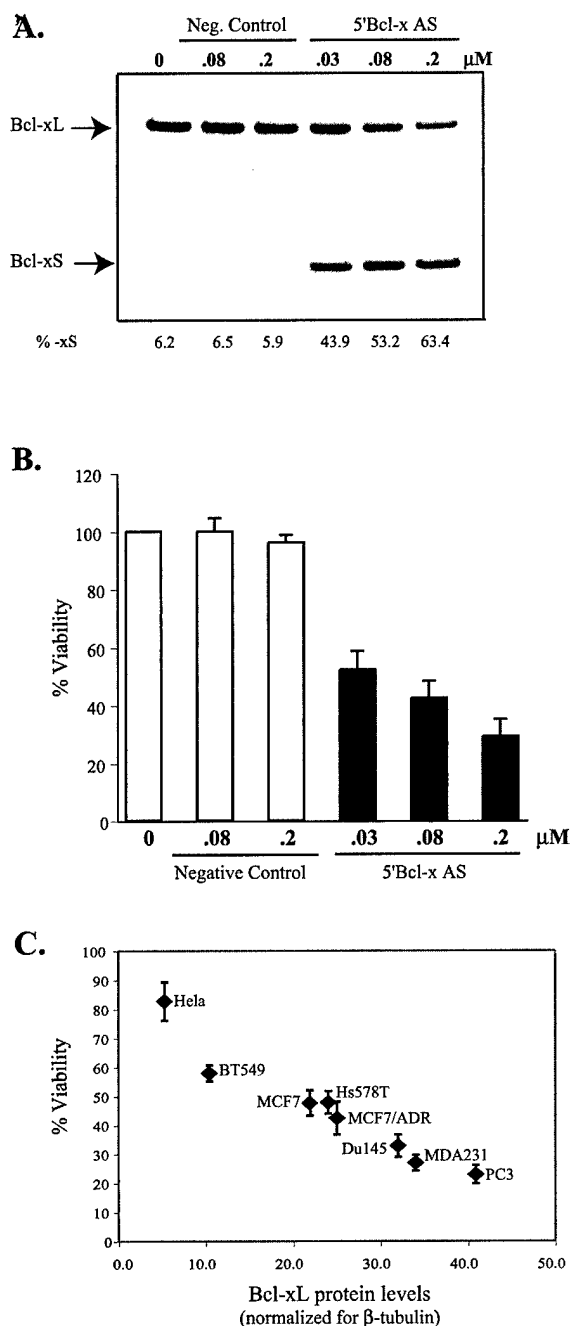


FIG. 8. Induction of cell death in MCF-7/ADR, multidrug-resistant breast cancer cell line by 5'Bcl-x AS. A, RT-PCR analysis of MCF-7/ADR cells transfected with increasing doses of 5'Bcl-x AS and control oligonucleotide. Percent of Bcl-xS is shown below each lane. B, clonogenic assay of control (open bars) and 5'Bcl-x AS-treated cells (black bars). Cell viability is expressed as percent colonies formed after oligonucleotide treatment versus mock-transfected cells. C, correlation of Bcl-xL protein levels (expressed in arbitrary units converted to a 0–50 unit scale) with viability of the cells treated with 5'Bcl-x AS at EC_{50,splicing}.

DISCUSSION

Several recent studies showed that antisense oligonucleotide-mediated down-regulation of expression of Bcl-xL and other anti-apoptotic genes enhanced apoptosis with and without additional treatment with chemotherapeutic drugs (13, 18, 42–47). In these approaches, the higher the expression of the target mRNA, the less effective were the oligonucleotides. In the work reported here, the opposite was true; the higher the expression of Bcl-xL, the more pronounced the effects of the

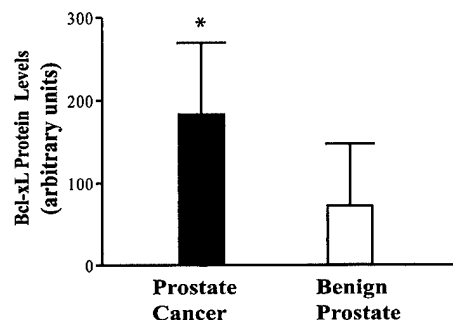


FIG. 9. Expression of Bcl-xL in human prostate cancer and benign prostate. Total protein from 10 cancer and 10 benign prostate tissue specimens were analyzed for Bcl-xL content by Western blotting with Bcl-x antibody. The intensities of the resulting Bcl-xL bands were quantified and normalized versus β -tubulin (see "Experimental Methods"). Asterisk, statistically significant difference from benign tissue ($p = .0012$; 95% CI; 2-tailed Student's t test).

5'Bcl-x AS oligonucleotide. These results show the power of oligonucleotide modification of splicing and bode well for the specificity of this approach.

The main advantage of splicing modification, especially in the context of opposing Bcl-xL and -xS splice variants, is that for every pre-mRNA molecule targeted with the antisense oligonucleotide one molecule of anti-apoptotic Bcl-xL is replaced with one molecule of pro-apoptotic Bcl-xS. The observations that antisense down-regulation of Bcl-xL was not very effective (23), or even promoted chemoresistance in some cases (48), suggest that the key contributor to 5'Bcl-x AS oligonucleotide-induced apoptosis was newly generated Bcl-xS. Importantly, as shown here, this splice variant was effective regardless of the expression profile of the targeted cells. This notion is well illustrated by the lack of correlation of 5'Bcl-x AS-induced cell death with the levels of Bcl-2, Bak, Bax, Mcl-1 apoptosis genes, p53 status, estrogen receptor status (for breast cancer cells), and *mdr1* gene expression (MCF-7/ADR cells). Apparent lack of impact of estrogen receptor status is particularly interesting since estradiol, acting via estrogen receptors, has been shown to activate anti-apoptotic pathways (49). Here, treatment of MCF-7 ER-positive breast cancer cells and Hs578T ER-negative breast cancer cells with equivalent doses of 5'Bcl-x AS resulted in similar levels of cell death. Furthermore, previous results showed that culturing MCF-7 cells in estradiol-free media did not enhance the apoptotic effects of 5'Bcl-x AS treatment (23). Thus, it appears that high expression of Bcl-xS is able to override several different anti-apoptotic pathways. These findings may be exploited as a prognostic tool to identify tumors that are most likely to benefit from 5'Bcl-x AS treatment. It is therefore encouraging that prostate cancer has higher levels of Bcl-xL compared with benign prostate (Fig. 9) or lower grade tumors (50). Furthermore, 5'Bcl-x AS should be quite specific as a drug since non-cancerous cells, that typically express low levels of Bcl-xL, should be relatively resistant to the treatment. While data presented in this paper suggest that the endogenous level of Bcl-xL is a major factor in several cell lines, the role of other factors in different cell lines cannot be ruled out. For example, cells may degrade the oligonucleotide faster, have different rates of mRNA turnover, varying expression levels of other apoptotic genes (such as caspases), or varying levels of proteins in pathways that interact with Bcl-xL and/or Bcl-xS function (e.g. PKC- and MEK-dependent pathways that regulate Bcl-xL expression, Refs. 51 and 52, and JNK, which phosphorylates Bcl-xL, Ref. 49).

The oligonucleotide-induced shift in splicing alone was able to cause significant cell death in PC3 cells and was even more effective in combination with chemotherapeutic agents, partic-

ularly with cisplatin and 5-FdU. Similarly, in MCF-7 cells the combination of cisplatin, 5-FdU, or doxorubicin with 5'Bcl-x AS oligonucleotide was more effective than each agent alone. This sensitization of cells indicates that in clinical treatments the concentration of the toxic antineoplastic agents can be lowered up to 10-fold if, for example, the results with PC3 cells and cisplatin and 5-FdU could be recapitulated in prostate cancer patients. Since in clinical trials, similarly modified oligonucleotides were found to be relatively non-toxic (53, 54), overall toxicity of the treatment would be reduced.

The specific mechanisms responsible for frequently observed variations in the degree of sensitization to the different chemotherapeutic agents (55, 56) are not entirely clear. The five tested chemotherapeutic drugs, as well as radiation, damage DNA and induce apoptosis (57, 58). Yet, they varied in the ways they acted in combination with 5'Bcl-x AS treatment. For example 5' Bcl-x AS treatment effectively sensitized the cells to 5-FdU but not to 5-FU. The obvious difference between these two drugs is that although both compounds incorporate into DNA and affect its function, 5-FU is also incorporated into RNA where it interferes with several processes including splicing (59). To follow this lead, we have tested the effects of all the drugs on the shift in splicing of Bcl-xL to Bcl-xS. Neither 5-FU, nor for that matter the remaining drugs, had any clear effect on splicing of Bcl-x pre-mRNA, as determined by RT-PCR of total RNA of treated MCF-7 and PC3 cells (data not shown). On the other hand, higher sensitivity of MCF-7 (wild type p53) versus PC3 (mutant p53) cells to doxorubicin is consistent with the observation that doxorubicin is most effective in cells with wild type p53 (60). Even technical details such as order of addition of drugs may affect their interactions (61). For example, Kano *et al.* (62) found that in various cancer cell lines paclitaxel and cisplatin could have antagonistic or additive effects depending on the order of treatment. Evidently, the mechanisms underlying different effects of drug combinations are not readily discerned based on simple assumptions. Additional work, most likely based on the global assessment of gene expression of cells treated with drugs and antisense oligonucleotides afforded by microarray technology (63–65) will be needed.

The finding that the multidrug-resistant cell line, MCF-7/ADR, is equal to the parent MCF-7 cells in its response to newly spliced Bcl-xS is encouraging. It suggests that the Bcl-xL/xS-dependent apoptotic pathways were not altered in the resistant cell line. The result also suggests that in the clinical setting, resistance due to overexpression of the *mdr1* gene, may still be overcome with the antisense therapy or that initial combination therapy may reduce the probability of selection of resistant cells. 5'Bcl-x AS treatment was unable to sensitize the cells to doxorubicin (data not shown) indicating that, as expected for a sequence-specific agent, the oligonucleotide did not affect the *mdr1* gene expression.

The fact that in MCF-7/ADR cells, the same reduction of viability as in parent MCF-7 cells was achieved at lower concentrations of 5'Bcl-x AS oligonucleotide suggests that its uptake was better in the doxorubicin-resistant cells. Experiments with fluorescent-labeled 2'-O-Me oligonucleotide confirmed that in these cells, there was higher nuclear accumulation of the oligonucleotide (data not shown). Questions remain as to whether there is a connection between this phenomenon and overexpression of *mdr1* or other means of drug resistance. Likewise, investigation of the uptake of other modified oligonucleotides, which appear to be more effective than 2'-O-Me derivatives (66), into MCF-7/ADR or other *mdr1*-overexpressing cells would be worthwhile. Positive answers to these questions would be very encouraging since the resistance of cancer cells to apoptosis induced by chemotherapeutic agents is a

major obstacle that impairs the effective treatment of many cancers.

The finding that cells that express higher levels of Bcl-xL were more sensitive to 5'Bcl-x AS-induced cell death, suggests that cancers that express high levels of Bcl-xL may benefit from treatment with the oligonucleotide. In particular, the effects of 5'Bcl-x AS combined with chemotherapeutic agents may be translated to clinical prostate cancer since recurrent prostate cancer expresses high levels of Bcl-xL. The potential combination of 5'Bcl-x AS with standard anti-cancer treatments warrants further exploration, especially in recurrent prostate cancer.

Acknowledgments—We thank our colleagues from UNC, Drs. Adrienne Cox and Nicole King for help with the UV experiments, Dr. Channing Der and Aylin Ulku for the MDA-MB 231 and BT549 cell lines, and Drs. Barry Goz and John Cidlowski (NIEHS) for reading this article. We thank Elizabeth Smith for technical assistance.

REFERENCES

- Han, J. S., Nunez, G., Wicha, M. S., and Clarke, M. F. (1998) *Springer Semin. Immunopathol.* **19**, 279–288.
- Lowe, S. W., and Lin, A. W. (2000) *Carcinogenesis* **21**, 485–495.
- Tannock, I. F., Osoba, D., Stockler, M. R., Ernst, D. S., Neville, A. J., Moore, M. J., Armitage, G. R., Wilson, J. J., Venner, P. M., Coppin, C. M., and Murphy, K. C. (1996) *J. Clin. Oncol.* **14**, 1756–1764.
- Savarese, D. M., Halabi, S., Hars, V., Akerley, W. L., Taplin, M. E., Godley, P. A., Hussain, A., Small, E. J., and Vogelzang, N. J. (2001) *J. Clin. Oncol.* **19**, 2509–2516.
- Kantoff, P. W., Halabi, S., Conaway, M., Picus, J., Kirshner, J., Hars, V., Trump, D., Winer, E. P., and Vogelzang, N. J. (1999) *J. Clin. Oncol.* **17**, 2506–2513.
- Amundson, S. A., Myers, T. G., Scudiero, D., Kitada, S., Reed, J. C., and Fornace, A. J., Jr. (2000) *Cancer Res.* **60**, 6101–6110.
- Sellers, W. R., and Fisher, D. E. (1999) *J. Clin. Invest.* **104**, 1655–1661.
- Reed, J. C. (1999) *J. Clin. Oncol.* **17**, 2941–2953.
- Olopade, O. I., Adeyanju, M. O., Safa, A. R., Hagos, F., Mick, R., Thompson, C. B., and Recant, W. M. (1997) *Cancer J. Sci. Am.* **3**, 230–237.
- Lebedeva, I., Rando, R., Ojwang, J., Cossum, P., and Stein, C. A. (2000) *Cancer Res.* **60**, 6052–6060.
- Minn, A. J., Rudin, C. M., Boise, L. H., and Thompson, C. B. (1995) *Blood* **86**, 1903–1910.
- Nita, M. E., Ono-Nita, S. K., Tsuno, N., Tominaga, O., Takenoue, T., Sunami, E., Kitayama, J., Nakamura, Y., and Nagawa, H. (2000) *Jpn. J. Cancer Res.* **91**, 825–832.
- Broome, H. E., Yu, A. L., Diccianni, M., Camitta, B. M., Monia, B. P., and Dean, N. M. (2002) *Leuk. Res.* **26**, 311–316.
- Boise, L. H., Gonzalez-Garcia, M., Postema, C. E., Ding, L., Lindsten, T., Turka, L. A., Mao, X., Nunez, G., and Thompson, C. B. (1993) *Cell* **74**, 597–608.
- Clarke, M. F., Apel, I. J., Benedict, M. A., Eipers, P. G., Sumantran, V., Gonzalez-Garcia, M., Doedens, M., Fukunaga, N., Davidson, B., Dick, J. E., and *et al.* (1995) *Proc. Natl. Acad. Sci. U. S. A.* **92**, 11024–11028.
- Ealovega, M. W., McGinnis, P. K., Sumantran, V. N., Clarke, M. F., and Wicha, M. S. (1996) *Cancer Res.* **56**, 1965–1969.
- Ohi, Y., Kim, R., and Toge, T. (2000) *Int. J. Oncol.* **16**, 959–969.
- Taylor, J. K., Zhang, Q. Q., Monia, B. P., Marcussen, E. G., and Dean, N. M. (1999) *Oncogene* **18**, 4495–4504.
- Sumantran, V. N., Ealovega, M. W., Nunez, G., Clarke, M. F., and Wicha, M. S. (1995) *Cancer Res.* **55**, 2507–2510.
- Kim, R., Ohi, Y., Inoue, H., and Toge, T. (1999) *Int. J. Oncol.* **15**, 751–756.
- Minn, A. J., Boise, L. H., and Thompson, C. B. (1996) *J. Biol. Chem.* **271**, 6306–6312.
- Fridman, J. S., Parsels, J., Rehemtulla, A., and Maybaum, J. (2001) *J. Biol. Chem.* **276**, 4205–4210.
- Mercatante, D. R., Bortner, C. D., Cidlowski, J. A., and Kole, R. (2001) *J. Biol. Chem.* **276**, 16411–16417.
- Taylor, J. K., Zhang, Q. Q., Wyatt, J. R., and Dean, N. M. (1999) *Nat. Biotechnol.* **17**, 1097–1100.
- Nieves-Neira, W., and Pommier, Y. (1999) *Int. J. Cancer* **82**, 396–404.
- Cattaneo-Pangrazzi, R. M., Schott, H., Wunderli-Allenspach, H., Rothen-Rutishauser, B., Guenther, M., and Schwendener, R. A. (2000) *J. Cancer Res. Clin. Oncol.* **126**, 247–256.
- Carroll, A. G., Voeller, H. J., Sugars, L., and Gelmann, E. P. (1993) *Prostate* **23**, 123–134.
- Kalkhoven, E., Roelen, B. A., de Winter, J. P., Mummery, C. L., van den Eijnden-van Raaij, A. J., van der Saag, P. T., and van der Burg, B. (1995) *Cell Growth & Differ.* **6**, 1151–1161.
- Shao, Z. M., Shen, Z. Z., Fontana, J. A., and Barsky, S. H. (2000) *Anticancer Res.* **20**, 2409–2416.
- Wei, Q., and Adelstein, R. S. (2002) *Mol. Biol. Cell* **13**, 683–697.
- Sierakowska, H., Sambade, M. J., Schumperli, D., and Kole, R. (1999) *RNA* **5**, 369–377.
- Strasberg Rieber, M., Zangemeister-Wittke, U., and Rieber, M. (2001) *Clin. Cancer Res.* **7**, 1446–1451.
- Vrana, J. A., Decker, R. H., Johnson, C. R., Wang, Z., Jarvis, W. D., Richon, V. M., Ehinger, M., Fisher, P. B., and Grant, S. (1999) *Oncogene* **18**,

- 7016-7025
34. Lee, J. U., Hosotani, R., Wada, M., Doi, R., Kosiba, T., Fujimoto, K., Miyamoto, Y., Tsuji, S., Nakajima, S., Nishimura, Y., and Imamura, M. (1999) *Eur. J. Cancer* **35**, 1374-1380
35. Zhan, Q., Alamo, I., Yu, K., Boise, L. H., Cherney, B., Tosato, G., O'Connor, P. M., and Fornace, A. J., Jr. (1996) *Oncogene* **13**, 2287-2293
36. Sakakura, C., Sweeney, E. A., Shirahama, T., Igarashi, Y., Hakomori, S., Nakatani, H., Tsujimoto, H., Imanishi, T., Ohgaki, M., Ohyama, T., Yamazaki, J., Hagiwara, A., Yamaguchi, T., Sawai, K., and Takahashi, T. (1996) *Int. J. Cancer* **67**, 101-105
37. Ogretmen, B., and Safa, A. R. (1996) *Int. J. Cancer* **67**, 608-614
38. Bendorra, Z., Trussardi, A., Morjani, H., Villa, A. M., Doglia, S. M., and Manfait, M. (2000) *E. J. Cancer* **36**, 428-434
39. Fairchild, C. R., Ivy, S. P., Kao-Shan, C. S., Whang-Peng, J., Rosen, N., Israel, M. A., Melera, P. W., Cowan, K. H., and Goldsmith, M. E. (1987) *Cancer Res.* **47**, 5141-5148
40. Schneider, E., Yamazaki, H., Sinha, B. K., and Cowan, K. H. (1995) *Br. J. Cancer* **71**, 738-743
41. Schneider, E., Horton, J. K., Yang, C. H., Nakagawa, M., and Cowan, K. H. (1994) *Cancer Res.* **54**, 152-158
42. Leech, S. H., Olie, R. A., Gautschi, O., Simoes-Wust, A. P., Tschopp, S., Haner, R., Hall, J., Stahel, R. A., and Zangemeister-Wittke, U. (2000) *Int. J. Cancer* **86**, 570-576
43. Xu, Z., Friess, H., Solioz, M., Aebi, S., Korc, M., Kleeff, J., and Buchler, M. W. (2001) *Int. J. Cancer* **94**, 268-274
44. Fennell, D. A., Corbo, M. V., Dean, N. M., Monia, B. P., and Cotter, F. E. (2001) *Br. J. Haematol.* **112**, 706-713
45. Gautschi, O., Tschopp, S., Olie, R. A., Leech, S. H., Simoes-Wust, A. P., Ziegler, A., Baumann, B., Odermatt, B., Hall, J., Stahel, R. A., and Zangemeister-Wittke, U. (2001) *J. Natl. Cancer Inst.* **93**, 463-471
46. Olie, R. A., and Zangemeister-Wittke, U. (2001) *Drug Resist. Update* **4**, 9-15
47. Miyake, H., Hara, I., Kamidono, S., and Gleave, M. E. (2001) *Int. J. Urol.* **8**, 337-349
48. Vilenchik, M., Raffo, A. J., Benimetskaya, L., Shames, D., and Stein, C. A. (2002) *Cancer Res.* **62**, 2175-2183
49. Razandi, M., Pedram, A., and Levin, E. R. (2000) *Mol. Endocrinol.* **14**, 1434-1447
50. Krajewska, M., Krajewski, S., Epstein, J. I., Shabaik, A., Sauvageot, J., Song, K., Kitada, S., and Reed, J. C. (1996) *Am. J. Pathol.* **148**, 1567-1576
51. Tsushima, H., Urata, Y., Miyazaki, Y., Fuchigami, K., Kuriyama, K., Kondo, T., and Tomonaga, M. (1997) *Cell Growth & Differ.* **8**, 1317-1328
52. Pardo, O. E., Arcaro, A., Salerno, G., Raguz, S., Downward, J., and Seckl, M. J. (2002) *J. Biol. Chem.* **277**, 22980-22984
53. Bennett, C. F. (1999) *Exp. Opin. Invest. Drugs* **8**, 237-253
54. Dorr, F. A., Glover, J. G., and Kwok, T. J. (2001) in *Antisense Drug Technology: Principles, strategies, and applications* (Crooke, S. T., ed), pp. 269-290, Marcel Dekker, Inc., New York
55. Dole, M. G., Jasty, R., Cooper, M. J., Thompson, C. B., Nunez, G., and Castle, V. P. (1995) *Cancer Res.* **55**, 2576-2582
56. Yang, C. C., Hsu, C. P., and Yang, S. D. (2000) *Clin. Cancer Res.* **6**, 1024-1030
57. Mesner, P., Budihardjo, I., and Kaufmann, S. (1997) *Adv. Pharmacol.* **41**, 461-499
58. Katzung, B. G. (1998) *Basic and Clinical Pharmacology*, 7th Ed., pp. 881-915, Appleton and Lange, Stamford, CT
59. Ghoshal, K., and Jacob, S. T. (1997) *Biochem. Pharmacol.* **53**, 1569-1575
60. Blagosklonny, M. V. (2001) *Leukemia* **15**, 869-874
61. Peters, G. J., van der Wilt, C. L., van Moorsel, C. J., Kroep, J. R., Bergman, A. M., and Ackland, S. P. (2000) *Pharmacol. Ther.* **87**, 227-253
62. Kano, Y., Akutsu, M., Tsunoda, S., Suzuki, K., and Yazawa, Y. (1996) *Cancer Chemother. Pharmacol.* **37**, 525-530
63. Mercatante, D. R., and Kole, R. (2002) *Biochim. Biophys. Acta* **1587**, 126-132
64. Fisher, A. A., Ye, D., Sergueev, D. S., Fisher, M. H., Shaw, B. R., and Juliano, R. L. (2002) *J. Biol. Chem.* **277**, 22980-22984
65. Cho, Y. S., Kim, M. K., Cheadle, C., Neary, C., Becker, K. G., and Cho-Chung, Y. S. (2001) *Proc. Natl. Acad. Sci. U. S. A.* **98**, 9819-9823
66. Sazani, P., Kang, S. H., Maier, M. A., Wei, C., Dillman, J., Summerton, J., Manoharan, M., and Kole, R. (2001) *Nucleic Acids Res.* **29**, 3965-3974

Identification of Differentially Expressed Genes Associated With Androgen-Independent Growth of Prostate Cancer

James L. Mohler,^{1,2,4*} Tammy L. Morris,⁴ O. Harris Ford III,⁴ Rudolf F. Alvey,⁴ Choitsu Sakamoto,⁵ and Christopher W. Gregory^{1,3}

¹Department of Surgery (Division of Urology), University of North Carolina-Chapel Hill, Chapel Hill, North Carolina

²Department of Pathology and Laboratory Medicine, University of North Carolina-Chapel Hill, Chapel Hill, North Carolina

³Department of Pediatrics (Laboratories for Reproductive Biology), University of North Carolina-Chapel Hill, Chapel Hill, North Carolina

⁴University of North Carolina-Lineberger Comprehensive Cancer Center, University of North Carolina-Chapel Hill, Chapel Hill, North Carolina

⁵Third Department of Internal Medicine, Nippon Medical School, Tokyo, Japan

BACKGROUND. The human prostate cancer xenograft, CWR22, similar to most human prostate cancers, regresses after castration and recurs several months after the removal of androgen. Genes uniquely associated with proliferation were identified by comparison of tumors that exist in androgen absence but differ in proliferative capacity.

METHODS. cDNA libraries from CWR22 tumors from 20-day castrate mice (proliferation undetectable) and recurrent CWR22 tumors (proliferation rate similar to androgen-dependent CWR22) were compared to evaluate the possibility that proliferation is triggered by either gain of function or loss of suppression. Differentially expressed genes were evaluated further for their temporal association with the onset of cellular proliferation using northern and western analysis and immunohistochemistry of a series of CWR22 tumors that spanned the transition from androgen-dependent to recurrent growth.

RESULTS. Subtractive hybridization identified 11 candidate genes from among 1,057 clones examined. Northern analysis confirmed differential expression of 8 genes. Western analysis revealed an association between tomoregulin, translation elongation factor-1 α (EF-1 α), Mxi-1, and thioredoxin-binding protein 2/vitamin D up-regulated protein, and the onset of recurrent growth. Immunohistochemistry revealed expression of tomoregulin, EF-1 α , Mxi-1, and thioredoxin reductase-1 coincidental with the onset of cellular proliferation on day 120 after castration.

CONCLUSIONS. One or more of these genes may represent an appropriate target to prevent, delay or treat recurrent prostate cancer. *Prostate* 51: 247–255, 2002. © 2002 Wiley-Liss, Inc.

KEY WORDS: gene expression; subtractive hybridization; prostate cancer xenograft; cellular proliferation

Grant sponsor: Department of Defense Prostate Cancer Research Program; Grant number: DAMD 98-8538; Grant sponsor: National Cancer Institute; Grant number: PO1-CA-77739.

*Correspondence to: Dr. James L. Mohler, Department of Surgery (Division of Urology), Pathology and Laboratory Medicine, and the University of North Carolina-Lineberger Comprehensive Cancer

Center, Campus Box 7235, University of North Carolina-Chapel Hill, Chapel Hill, NC 27599. E-mail: jlmohler@med.unc.edu
Received 4 October 2001; Accepted 24 January 2002
Published online 25 April 2002 in Wiley InterScience
(www.interscience.wiley.com). DOI 10.1002/pros.10086

INTRODUCTION

An American man is diagnosed with prostate cancer (CaP) every 3 min and dies from the disease every 17 min [1]. Although increased public awareness of CaP and use of early detection strategies employing serum prostate-specific antigen (PSA) has increased the frequency of detection and treatment of organ-confined CaP, many men still present with advanced CaP or suffer recurrence after potentially curative therapy. For these men, CaP may be palliated with androgen deprivation therapy. CaP undergoes apoptosis and regression following androgen deprivation but recurs despite the absence of testicular androgens. Many investigators are comparing androgen-dependent and recurrent CaP in clinical specimens or cell lines using molecular approaches. These experiments may identify many genes whose expression is altered, only a few of which are critical for the development of recurrent growth.

The CWR22 human CaP xenograft retains the biological characteristics exhibited by most human CaPs, including regression following castration and recurrence several months after the removal of androgen [2–4]. Previous reports described mRNA transcripts that were identified using differential expression analysis that were down-regulated in androgen-withdrawn CWR22 but up-regulated in recurrent CWR22 despite the continued absence of androgen [5,6].

Our hypothesis is that the onset of CaP cellular proliferation after castration is associated with critical changes in gene expression that provide a novel target for therapy. We used subtracted cDNA libraries to identify genes uniquely associated with cellular proliferation in the CWR22 model by comparing non-proliferating and proliferating tumors. Differentially expressed genes were evaluated for temporal association with the onset of recurrent cellular proliferation using northern and western analyses and immunohistochemistry.

MATERIALS AND METHODS

Transplantation of CWR22 Tumors

Nude mice were purchased from Harlan Sprague Dawley, Inc., Indianapolis, IN. One million cells suspended in Matrigel[®] (Collaborative Research Inc., Bedford, MA) were injected subcutaneously into nude mice 4–5 weeks of age. A 12.5 mg sustained-release testosterone pellet (Innovative Research of America, Sarasota, FL) was placed subcutaneously in each animal 2 days before tumor injection and every 3 months thereafter to maintain consistent serum levels of testosterone of approximately 4 ng/ml. After tumors reached volume 1 cm³, animals were castrated

and testosterone pellets removed. Intact mice bearing tumors and castrated animals with either regressed or recurrent CWR22 tumors were sacrificed by cervical dislocation and tumors were resected and immediately frozen under liquid nitrogen or fixed in formalin and embedded in paraffin. For cDNA library construction, CWR22 tumors were obtained from four mice on day 20 after castration (no cellular proliferation), four 20-day castrate mice treated with subcutaneous testosterone propionate (TP) 1 mg/mouse for 48 hr and six mice 5 mo after castration (recurrent CWR22) (increased cellular proliferation).

RNA Isolation

Total RNA was isolated from 20-day castrate CWR22 and recurrent CWR22 using guanidine-thiocyanate and ultracentrifugation through a CsCl cushion [7]. Poly (A) mRNA was purified from total RNA using Oligotex mRNA Midi Spin-Columns and the manufacturer's protocol (Qiagen Inc., Valencia, CA). The quality of total RNA and poly (A) mRNA was confirmed using northern blot analysis [8].

cDNA Library Construction

Two µg of poly (A) mRNA from CWR22 tumors from 20-day castrate mice, recurrent CWR22 tumors from 150-day castrate mice and human skeletal muscle (control) were used to perform three subtractive hybridizations. One subtraction enriched for genes overexpressed in recurrent CWR22 tumors compared to CWR22 tumors from 20-day castrate mice and the second subtraction identified genes suppressed in recurrent CWR22 tumors compared to CWR22 tumors from 20-day castrate mice. Both subtractions and the control subtraction were performed using the PCR-Select cDNA Subtraction Kit (Clontech, Palo Alto, CA) and the manufacturer's directions. PCR products were amplified using thermal cycling conditions: 94°C for 30 sec, 66°C for 30 sec, and 72°C for 1.5 min for 27 cycles (initial) and 11 cycles (nested PCR). The average PCR product insert size was 0.5 kb as determined by agarose gel electrophoresis. PCR products were purified using QIAquick PCR Purification Kit (Qiagen Inc.). Purified nested PCR products from each subtracted cDNA library were ligated separately into the pGEM-T Easy Vector System 11 (Promega Corp., Madison, WI) and transformed into JM109 high efficiency competent cells (Promega Corp.). Transformed cells were plated on Luria-Bertani/Ampicillin/5-bromo-4-chloro-3-indolyl β-D-galactopyranoside/isopropyl β-D-thiogalactopyranoside plates. Plasmids containing inserts were identified using blue/white screening and DNA was prepared from white colonies.

cDNA Library Screening

DNA samples were diluted in 1.0 M Tris-EDTA, pH 8.0 (TE), and denatured in 3.6 M NaOH/90 mM EDTA (final 0.4 M NaOH/10 mM EDTA), incubated 10 min at 90°C and transferred to ice. DNA samples (420 µl) were blotted onto Zeta Probe[®] nylon membranes (Bio-Rad Laboratories, Hercules, CA) using a vacuum manifold apparatus. Two controls were included; a religated vector served as negative control and glyceraldehyde phosphate dehydrogenase (GAPDH) cDNA served as positive control. Multiple membranes were prepared in duplicate, UV cross-linked and rinsed in 2 × standard sodium citrate (SSC) for 30 sec. Slot blot membranes were pre-hybridized in 10 ml hybridization solution (5 × SSC, 5 × Denhardt's, 1% sodium dodecyl sulfate [SDS] and 100 µg/ml salmon sperm DNA) at 68°C for 60 min. 1 µg of poly (A) mRNA from CWR22 tumors from 20-day castrate mice and recurrent CWR22 tumors was radiolabeled as first strand cDNA by random priming with ³²P-dCTP, heat denatured, mixed with hybridization solution at 10 cpm/l, and hybridized to the membrane at 68°C overnight. After hybridization, blots were washed in 2 × SSC, 0.1% SDS followed by 1 hr at 50°C in 0.1 × SSC, 0.1% SDS. After washing, membranes were exposed to X-ray film (Eastman Kodak Co., Rochester, NY) with an intensifying screen at -80°C. Autoradiographs of duplicate blots hybridized to recurrent CWR22 and 20-day castrate CWR22 probes were then analyzed to identify bands resulting from differential hybridization to the two probes.

DNA Sequencing

Differentially expressed clones were amplified with M13 forward (5' TGTAACACGACGGCCAGT 3') and M13 reverse (5' CAGGAAACAGCTATGAC 3') primers using thermal cycling conditions: 95°C for 8 min (hot start), 94°C for 1 min, 55°C for 1 hr 30 min, 72°C for 2 min for 30 cycles followed by a 72°C 10 min extension. DNAs were purified using Microcon Centrifugal Filter Devices (Millipore Corporation, Bedford, MA) and sequenced by the University of North Carolina-Chapel Hill Automated DNA Sequencing Facility on a Model 377 DNA Sequencer (Perkin Elmer, Applied Biosystems Division, Foster City, CA) using the ABI PRISM[™] Dye Terminator Cycle Sequencing Ready Reaction Kit with AmpliTaq DNA Polymerase, FS (Perkin Elmer). DNA sequences were analyzed using Genetics Computer Group software (Wisconsin Package Version 10.2, Genetics Computer Group, Madison, WI) and compared to sequences in Gen-Bank (National Center for Biotechnology Information, Bethesda, MD).

Northern Analysis

DNAs from the 11 candidate genes were amplified with T7/SP6 primers (Promega Corp.) using thermal cycling conditions 95°C for 8 min, 94°C for 1 min, 46°C for 1 min, and 72°C for 1 min 30 sec for 30 cycles followed by a 10 min extension at 72°C. PCR products were purified using microspin filter tubes (Whatman, Markon, WA). Ten µg of total RNA each from androgen-dependent CWR22 tumors, CWR22 tumors from 20-day castrate mice, CWR22 tumors from 20-day castrate mice treated with TP 48 hr, and recurrent CWR22 were glycosylated and fractionated through 1% agarose gels and transferred to Biotrans nylon neutral membrane (ICN Biomedicals, Inc, Aurora, OH). Purified cDNA (12.5 ng) was labeled with [³²P]-dCTP (Amersham Corp., Arlington Heights, IL) by random priming (Boehringer Mannheim, Indianapolis, IN). Membranes were hybridized in aqueous solution (5 × SSC, 5 × Denhardt solution, 1% SDS, and 100 µg/ml salmon sperm DNA) overnight at 68°C. After washing at 50°C for 1 hr in 0.1 × SSC, 0.1% SDS, the membranes were exposed to X-ray film (Eastman Kodak Co., Rochester, NY) with an intensifying screen at -80°C. Quantitation of mRNA transcript levels was performed by scanning Northern blots with an Ultrosan XL Densitometer (LKB, Uppsala, Sweden). RNA loading differences were normalized by scanning the same blots subsequently hybridized with an 18S ribosomal RNA cDNA.

Western Analysis

Frozen androgen-stimulated CWR22 tumors, recurrent CWR22 tumors, and tumors from various intervals after castration (100 mg) were pulverized in liquid nitrogen, allowed to thaw on ice, and mixed with 1.0 ml of radioimmunoprecipitation assay (RIPA) buffer with protease inhibitors (PBS, 1% NP40, 0.5% sodium deoxycholate, 0.1% SDS, 0.5 mM phenylmethylsulfonyl fluoride, 10 µM pepstatin, 4 µM aprotinin, 80 µM leupeptin, and 5 mM benzamide). Tissue was homogenized on ice for 30 sec using a Biohomogenizer (Biospec Products, Inc., Bartlesville, OK), 2 µl of 0.2 M phenylmethylsulfonyl fluoride was added and homogenates were incubated 30 min on ice. Lysates were centrifuged at 10,000g for 20 min and supernatants were collected and centrifuged again to prepare final lysates. Supernatant protein (100 µg) from each sample was electrophoresed in 12% SDS-polyacrylamide gels, electroblotted to Immobilon-P membrane (Millipore Corp., Bedford, MA) and immunodetected. Antibodies were available for tomodulin [9] and purchased for thioredoxin reductase-1, a member of the thioredoxin-binding protein 2/vitamin D up-regulated protein TBP2 family (TBP2)

for which antibodies are commercially available (Upstate Biotechnology, Lake Placid, NY), and translation elongation factor-1 α (EF-1 α) (Upstate Biotechnology). Tomoregulin and thioredoxin reductase-1 monoclonal antibodies were used at 1:2,500 dilution and EF-1 α monoclonal antibody was used at 1:5,000 dilution. A mouse monoclonal and a goat polyclonal antiserum raised against Mxi-1 were used in Western blot analysis and created high backgrounds preventing the visualization of a specific Mxi-1 band. IgG was detected using goat-anti-mouse secondary antibody conjugated to horseradish peroxidase (Amersham Corp., Arlington Heights, IL) and enhanced chemiluminescence (DuPont NEN Research Products, Boston, MA). For protein loading controls, representative blots were stripped of antibody by incubating in 0.2 M NaOH for 20 min followed by incubation with anti-MAP kinase (ERK2) polyclonal antibody (Upstate Biotechnology, Lake Placid, NY) at 1:2,500 dilution.

Immunohistochemistry

Paraffin-embedded CWR22 tissue arrays were constructed that included all intervals after castration indicated above and appropriate controls. CWR22 tissue arrays were cut into 6 μ m-thick histologic sections. MIB-1 monoclonal antibody (Oncogene, Cambridge, MA) reacts with the cell cycle-associated antigen Ki-67 expressed during the proliferative phases (G1, S, G2, and M) but absent in the resting phase (G₀) of the cell cycle [10]. MIB-1 was diluted 1:50 and sections were incubated for 120 min at 37°C. Slides were incubated in biotinylated anti-mouse IgG (Vector Laboratories, Inc., Burlingame, CA) at 1:200 dilution and in horseradish peroxidase-conjugated avidin-biotin complex (ABC) (Vector) at 1:200 dilution. The immuno-peroxidase complexes were visualized using 0.75 mg/ml diaminobenzidine tetrahydrochloride (DAB) (Vector) for 8 min at 37°C. Colon cancer tissue served as positive controls and 0.5 μ g/ml non-immune mouse IgG was used instead of MIB-1 monoclonal antibody at the same IgG concentration for negative control slides prepared from the same tissue blocks as specimens; negative control slides were non-reactive. For tomoregulin, IHC was optimized [11] for standard sections using: AR 10 antigen retrieval solution (Biogenex, San Ramon, CA) in a vegetable steamer, M.O.M.TM (Vector Laboratories Inc., Burlingame, CA) to block mouse tissues adjacent to or part of CWR22 tumors, primary antibody at 1:800 dilution, biotinylated anti-mouse IgG at 1:200 dilution, ABC for detection and DAB for visualization. For EF-1 α and Mxi-1, conditions were the same except primary antibodies were used at 1:400 dilution. For thioredoxin reductase-1, IHC was optimized using citra antigen retrieval, primary antibody

at 1:600 dilution and biotinylated anti-rabbit IgG₁ at 1:200 dilution.

RESULTS

Subtractive Hybridization

cDNA libraries from CWR22 tumors from 20-day castrate mice (non-proliferating cells) and recurrent CWR22 tumors (proliferating cells) were compared using subtractive hybridization. Duplicate slot blots containing subtracted library DNAs were probed with radiolabeled first strand cDNA from CWR22 tumors from 20-day castrate mice and recurrent CWR22 tumors to evaluate differences in gene expression. A total of 1,057 clones were examined in two screenings of both subtracted libraries. Eleven DNAs representing differentially expressed genes were sequenced and compared with known gene sequences. Androgen receptor and glyceraldehyde-3-phosphate dehydrogenase were identified. Ten of the differentially expressed genes had homology to known transcripts identified previously: Mxi-1, a transcriptional regulator from the Myc family [12,13]; EF-1 α [14,15]; a human chromosome 3 gene that encodes an arginine-rich protein; tomoregulin [9]; carcinoembryonic antigen (CEA) [16]; TBP2 [17,18]; α 1 gene sequence with homology to sperm antigen-36 (HSA-36) [19]; MHC class III; tRNA synthetase and human ribosomal protein S10. One unknown gene had homology to DNA sequence on human chromosome 22.

Northern Analysis

Northern blot analysis using tumor RNAs from androgen-stimulated CWR22, CWR22 from 20-day castrate mice, CWR22 tumors from 20-day castrate + 48 hr TP and recurrent CWR22 tumors was used to confirm differential gene expression between tumors after short-term (20 days after castration = not proliferating in androgen absence) and long-term (150 days after castration = proliferating in androgen absence) castration (Fig. 1). Tomoregulin, EF-1 α , Mxi-1, HSA-36 and human ribosomal protein S10 were proliferation-associated and not androgen-regulated whereas TBP2, MCH class III and tRNA synthetase were both proliferation-associated and androgen-regulated. RNAs either increased slightly (MHC class III, tRNA synthetase, HSA-36) or 5-fold (tomoregulin, Mxi-1) in recurrent tumors compared with tumor RNA from 20 day castrated mice. Other RNAs decreased slightly (EF-1 α , human ribosomal protein S10) or 75% (TBP2) when recurrent CWR22 tumors were compared to tumors from 20-day castrate CWR22 mice. MHC class III and tRNA synthetase RNAs increased 2-fold and TBP2 RNA decreased 2-fold when 20-day castrate

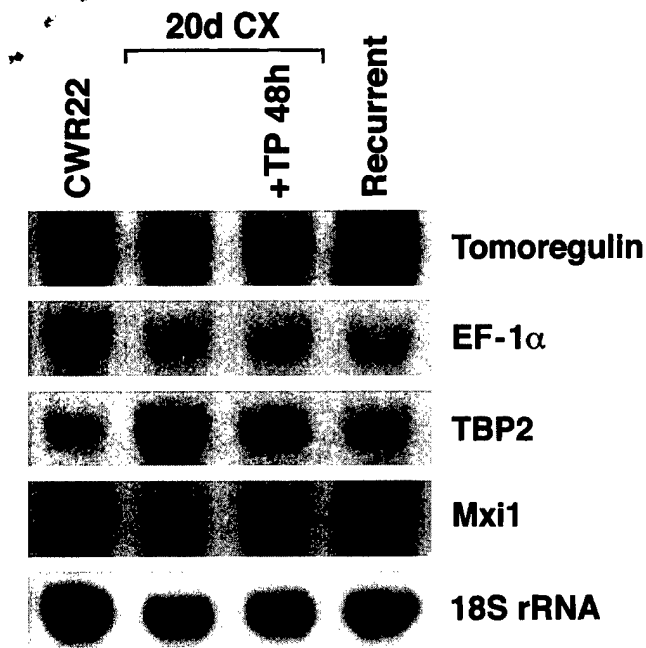


Fig. 1. Northern blot analysis of gene expression in CWR22 tumors. Total RNA (10 µg/lane) extracted from CWR22 tumors was analyzed by Northern blot analysis on 1.0% agarose gels, using PCR fragments of the DNAs of interest labeled with [³²P]dCTP. CWR22, CWR22 tumors from intact male mice; 20d CX, CWR22 tumors from 20-day castrate mice; TP, testosterone propionate; recurrent, CWR22 tumors 5 months after castration. 18S rRNA was used as a loading control. Results are representative of two independent experiments.

CWR22 tumors were stimulated with 48 hr TP. Thus, of 11 candidate genes identified using subtractive hybridization, Northern analysis confirmed 8 genes were temporally associated with cellular proliferation in the CWR22 model, of which 3 were androgen-regulated (MHC class III, tRNA synthetase, and TBP2) and 5 were not changed with androgen treatment (human ribosomal protein S10, HSA-36, tomoregulin, EF-1α, and Mxi-1).

Western Analysis

Tomoregulin expression was highest in androgen-stimulated and recurrent CWR22 tumors and increased after 48 hr TP treatment of 6-day castrate mice (Fig. 2). EF-1α protein levels were reduced on day 12 after castration and remained low on day 32 after castration (not shown). EF-1α levels in recurrent CWR22 were similar to those in androgen-stimulated CWR22. Thioredoxin reductase-1 protein levels in CWR22 tumors decreased slightly on day 6 after castration and increased 2 fold after TP treatment of a 6-day castrate mouse. Thioredoxin reductase-1 was barely detectable on days 12, 32, and 64 after castration and remained low in recurrent CWR22

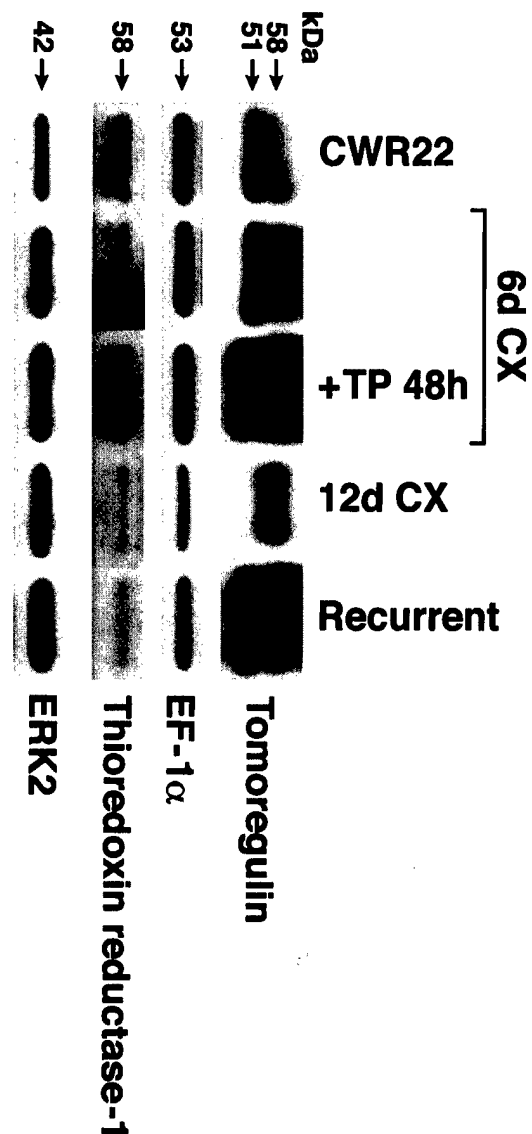


Fig. 2. Immunoblot analysis of CWR22 tumor lysates. 100 µg protein samples were separated by electrophoresis on 12% polyacrylamide gels and electroblotted to nitrocellulose membranes. Immunoblots were incubated with antibodies to tomoregulin, EF-1α, thioredoxin reductase-1, and MAP kinase ERK2. CWR22, tumors from intact male mice; 6d CX, CWR22 tumors from 6-day castrate mice; TP, testosterone propionate; 12d CX, CWR22 tumors from 12-day castrate mice; recurrent, CWR22 tumors 5 months after castration. The positions of molecular mass markers (kDa) are indicated. Results are representative of 2–3 independent experiments for each antibody.

tumor lysates. Due to nonspecific reactivity of Mxi-1 antibodies, Western blot results are not presented.

Immunohistochemistry

Immunohistochemistry for tomoregulin, EF-1α and thioredoxin reductase-1 confirmed northern and western analyses; selected images demonstrate these findings (Fig. 3). Expression of tomoregulin (Row 1),

EF-1 α (Row 2), Mxi-1 (Row 3) and thioredoxin reductase-1 (Row 4) was similar in androgen-stimulated (Column 3) and recurrent CWR22 (Column 6). Immunohistochemistry in CWR22 tumors for the 4 genes was similar to their expression in clinical specimens of androgen dependent CaP (Column 1) and recurrent CaP (Column 2). In CWR22 tumors, immunostaining for tomoregulin, EF1 α and Mxi-1 was reduced on day 20 after castration (Column 4). On day 120 after castration, tomoregulin and thioredoxin reductase-1 had increased immunostaining compared to tumors from 20 day castrated mice. Re-expression of these genes occurred coincidentally with the development of small foci of proliferating cells recognized using MIB-1 to immunostain Ki-67 antigen (Row 5).

DISCUSSION

Subtractive hybridization was used to identify 11 transcripts expressed in intact mice bearing CWR22 tumors and castrated mice bearing recurrent CWR22 tumors but not in regressed tumors. Northern analysis confirmed temporal association with tumor growth before and after castration for eight of these candidates: five that were proliferation-associated and not androgen-regulated (tomoregulin, EF-1 α , Mxi-1, HAS-36 and human ribosomal protein S10) and three that were proliferation-associated and androgen-regulated (TBP2, MHC class III, and tRNA synthetase). In order to evaluate these candidate genes further, antibodies were used for immunohistochemical comparison of protein expression and cellular localization during the transition from androgen-stimulated to recurrent CaP. In a previous study [20], we used MIB1 detection of Ki-67 and automated video image analysis of paraffin sections of CWR22 xenograft tumors obtained prior to and at intervals after castration until tumor recurrence to determine the onset of cellular proliferation after castration. Cellular proliferation was undetectable by image analysis until 120 days after castration when visual inspection revealed multiple foci of proliferating cells. The onset of cellular proliferation coincided with an increase ($P=0.01$) in serum PSA from 11.1 ± 1.8 ng/ml on day 90 after castration to 21.3 ± 4.1 ng/ml on day 120 after castration. In addition, the foci of proliferating cells expressed increased levels of PSA when adjacent sections were stained for Ki-67 and PSA. The appearance of proliferating tumor cells that expressed PSA 120 days after castration indicated that these foci might be the precursors of recurrent tumors. Therefore, further evaluation of candidate genes required Western and immunohistochemical comparison of proliferating CWR22 tumors prior to, 120 days after and upon recurrence after castration and non-proliferating CWR22 tumors regressed after castration.

In earlier studies, differential expression analysis was used to identify transcripts that were down-regulated upon castration but upregulated in recurrent CWR22 despite the continued absence of androgen [5]. Androgen-regulated mRNAs included Nkx3.1, human glandular kallikrein 2 (hK2), insulin-like growth factor binding protein-5 (IGFBP-5), α -tubulin, α -enolase and PSA, all of which were down-regulated in CWR22 following castration and up-regulated in recurrent CWR22 in the continued absence of androgen. IGFBP-5 expression was characterized further using Western blotting, ligand blotting, and immunohistochemistry that revealed IGFBP-5 was more highly expressed in CaP compared to benign prostatic hyperplasia (BPH) or high-grade prostatic intraepithelial neoplasia (PIN) [6]. Androgen regulation of cell cycle proteins CDK1 and CDK2, and cyclins A, B1, and D1 in CWR22 tumors was demonstrated using ribonuclease protection assays and Western blot analysis. CDK1:cyclin B1 and CDK4:cyclin D1 protein complex formation and Rb phosphorylation were also shown to be androgen regulated using co-immunoprecipitation and in vitro kinase assays, respectively [21]. We recently found that a majority of recurrent prostate cancers express high levels of two nuclear receptor coactivators, transcriptional intermediary factor 2 (TIF2) and steroid receptor coactivator 1 (SRC1). Overexpression of these coactivators increased AR transactivation at physiological concentrations of adrenal androgen [22]. Finally, RNAs were prepared from CWR22 tumors from intact mice, mice with recurrent tumors and mice on days 6 and 12 after castration. cDNA microarray screening (using the Atlas Human 1.2 Array, Clontech) identified approximately 250 (of 1,200) genes that are expressed differentially after castration or upon recurrence in CWR22 (unpublished data). In order to focus upon clinically relevant genes responsible for CaP recurrence after castration instead of the large number of androgen-regulated genes, we sought to identify genes uniquely associated with proliferation by comparison of tumors that exist in androgen absence but differ in proliferative capacity.

Of the eight candidate genes identified by subtractive hybridization and confirmed by northern analysis, two were expected to be associated generally with growth (ribosomal protein S10 and tRNA synthetase), one was conceptually unlikely to be growth-regulatory (MHC class III gene), one has only partial sequence known (HSA-36) and antibodies were not available for TBP2 gene products. The expression level of thioredoxin reductase-1 was examined since antibody was available to this downstream effector molecule in the thioredoxin-signaling pathway. Tomoregulin, EF-1 α and thioredoxin reductase-1 were

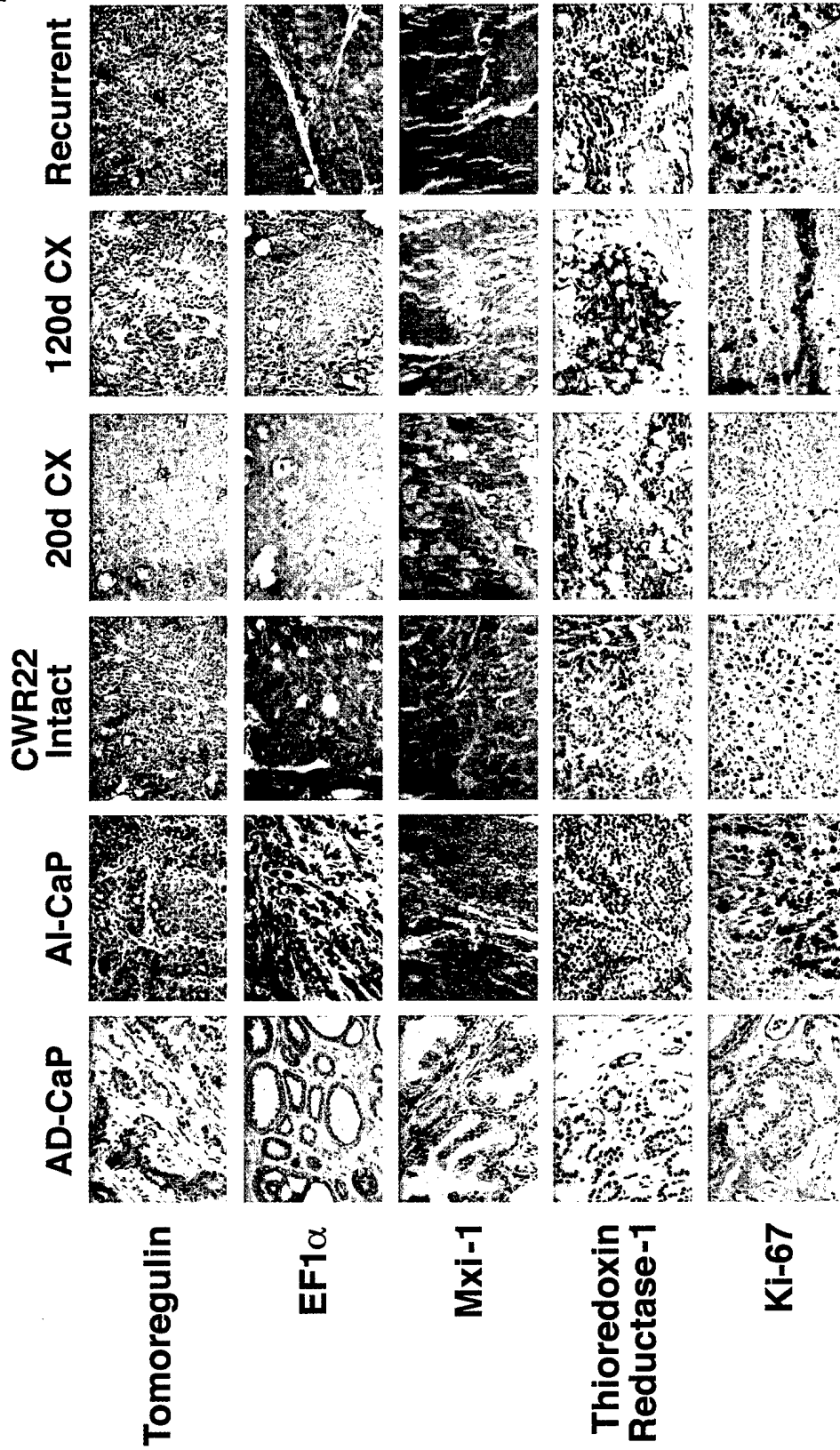


Fig. 3. Immunohistochemical analysis of paraffin-embedded human prostate cancer and CWR22 tumors. Clinical samples were selected from 5 men who underwent radical prostatectomy for clinically localized CaP and 5 men who underwent transurethral resection for urinary retention caused by CaP that recurred long after castration. CWR22 samples were selected from a tissue microarray constructed from 119 different tumors. AD-CaP, androgen-dependent prostate cancer; AI-CaP, androgen-independent (recurrent) prostate cancer; CWR22 intact, tumors from intact male mice; 20d CX, CWR22 tumors from 20-day castrate mice; 120d CX, CWR22 tumors from 120-day castrate mice; recurrent, CWR22 tumors 5 months after castration. Magnification, 200 \times .

expressed in CWR22 tumors on day 120 after castration, androgen-stimulated CWR22 and recurrent CWR22 but not in regressed tumors.

Tomoregulin, a novel EGF-like protein, was cloned from a stomach fibroblast cDNA library by screening for EGF-like domains of the EGF and neuregulin family [9]. Tomoregulin is expressed in gastric cancer cell lines, brain and gastric tissues and developing embryos at middle to late stages. Tomoregulin may have many functions; it may serve as a ligand for erbB-receptor, regulate TGF- β -related growth factor signaling and mediate cell signaling through G-protein activation. Tomoregulin's relevance to CaP, generally, and the development of androgen-independent growth, specifically, is suggested by its similarity to EGF. EGF is androgen-regulated, expressed in large amounts in both benign and malignant prostate tissues and fluids and is strongly mitogenic (reviewed in [23]). Immunohistochemical studies of clinical specimens have led to the suggestion that androgen-stimulated CaP may have a paracrine pattern of EGF and TGF- α stimulation whereas recurrent CaP may exhibit a shift toward autocrine growth factor loops [23]. In vitro studies using normal prostatic epithelial cells, the androgen-sensitive LNCaP and androgen-independent DU145 and PC3 human CaP cell lines have suggested that: (1) the EGF receptor is expressed and autophosphorylated at higher levels in DU145 and PC3 than LNCaP and normal epithelial cells and may contribute to androgen-independent growth [24]; (2) EGF and IGF-I activate intracellular signaling pathways that converge at MAPK p42/ERK2 that is constitutively activated in DU145 but not LNCaP [25]; and (3) blockade of the EGF receptor attenuates the actions of both EGF and IGF-I, acts through both the MAPK and PKA pathways, and may provide novel targets for treatment of recurrent CaP [26]. Our finding from Northern and Western analysis suggests that tomoregulin may be translationally regulated but not transcriptionally regulated by androgen. Increased tomoregulin protein expression in recurrent tumors and tumors from 6-day castrate mice treated with testosterone for 48 hr parallels the expression of androgen receptor [5,22]. This may result from stabilization of tomoregulin protein or decreased proteolysis in the presence of androgen. Antibody neutralization of the protein may be an effective method of preventing tomoregulin activity in prostate cancer.

EF-1 α has been shown to be an important regulator of the cell cycle and is over-expressed in tumor tissues [14]. Overexpression of EF-1 α caused several cell lines to become highly susceptible to chemical or ultraviolet light induced transformation [15]. EF-1 α has a truncated homologue in CaP known as prostate tumor inducing gene-1 (PTI-1) [27]. EF-1 α may be an im-

portant modulator of recurrent prostate cancer cell growth.

TBP2, cloned recently [17,18], was found identical to vitamin D-upregulated 1 protein that was originally reported as an up-regulated gene in HL-60 cells treated with 1, 25-dihydroxyvitamin D₃. The thiorodoxins (of which TBP2 is a member) are ubiquitous proteins that are important in regulation of cellular reduction and oxidation that impacts, among other things, DNA binding of transcription factors including steroid receptors [28,29], apoptosis [30,31] and differentiation [32].

Mxi-1 shares the pattern of expression of tomoregulin when evaluated by northern analysis. Mxi-1, a transcriptional regulator from the Myc family, was shown to be expressed in CaP and lack point mutations in microdissected cells [12]. Myc expression was shown to be elevated in CaP compared to BPH [13] and elevated mRNA and protein expression for Myc has been detected in recurrent CWR22 tumors (unpublished data).

Identification of critical genes associated with the onset of cellular proliferation after castration may provide novel targets for treatment aimed at prevention or delay of the onset of CaP recurrence after androgen deprivation therapy. Clinical trials are ongoing exploring agents that target growth factor receptors and cell signaling molecules. Greater specificity and hence lower toxicity may be possible by targeting individual genes and their products that are expressed at critical times in cancer progression. Our strategy has identified several gene targets, at least three of which warrant further investigation using more detailed immunohistochemical study of the onset of cellular proliferation at 120 days after castration in the CWR22 model and other androgen-responsive xenografts and in vitro testing using androgen-sensitive and androgen-independent cell lines for effects of gene manipulation. Further study may yield candidates for manipulation using antisense therapy that can be tested in the CWR22 model prior to investigation in human patients to prevent or delay recurrent CaP.

ACKNOWLEDGMENTS

We greatly appreciate the technical assistance of Natalie Edmund, Katherine Hamil, and Raymond T. Johnson.

REFERENCES

1. Greenlee RT, Hill-Harmon MB, Murray T, Thun M. Cancer Statistics. *CA Cancer J Clin* 2001;51:15-36.
2. Pretlow TG, Wolman SR, Micale MA, Pelley RJ, Kursh ED, Resnick MI, Bodner DR, Jacobberger JW, Delmoro CM, Giaconia JM, Pretlow TP. Xenografts of primary human prostatic carcinoma. *J Natl Cancer Inst* 1993;85:394-398.

3. Wainstein MA, He F, Robinson D, Kung H-J, Schwartz S, Giaconia JM, Edgehouse NL, Pretlow TP, Bodner DR, Kursh ED, Resnick MI, Amini SB, Pretlow TG. CWR22: Androgen-dependent xenograft model derived from a primary human prostatic carcinoma. *Cancer Res* 1994;54: 6049-6052.
4. Nagabhushan M, Miller CM, Pretlow TP, Giaconia JM, Edgehouse NL, Schwartz S, Kung H-J, de Vere White RW, Gumerlock PH, Resnick MI, Amini SB, Pretlow TG. CWR22: the first human prostate cancer xenograft with strong androgen-dependent and relapsed stains both in vivo and soft agar. *Cancer Res* 1996;56:3042-3046.
5. Gregory CW, Hamil KG, Kim D, Hall SH, Pretlow TG, Mohler JL, French FS. Androgen receptor expression in androgen-independent prostate cancer is associated with increased expression of androgen-regulated genes. *Cancer Res* 1998;58: 5718-5724.
6. Gregory CW, Kim D, Ye P, D'Ecole AJ, Pretlow TG, Mohler JL, French FS. Androgen receptor up-regulates insulin-like growth factor binding protein-5 (IGFBP-5) expression in a human prostate cancer xenograft. *Endocrinology* 1999;40: 2372-2381.
7. Chirgwin JM, Przbyla AE, MacDonald RJ, Rutter WJ. Isolation of biologically active ribonucleic acid from sources enriched in ribonuclease. *J Am Chem Soc* 1979;78:5294-5299.
8. Pederson T, Davis NG. Messenger RNA processing and nuclear structure: isolation of nuclear ribonucleoprotein particles containing beta-globin messenger RNA precursors. *J Cell Biol* 1980; 87:47-54.
9. Uchida T, Wada K, Akamatsu T, Yonezawa M, Hitoshi N, Mizoguchi A, Kasuga M, Sakamoto C. A novel epidermal growth factor-like molecule containing two follistatin modules stimulates tyrosine phosphorylation of erbB-4 in MKN28 gastric cancer cells. *Biochem Biophys Res Comm* 1999;266: 593-602.
10. Gerdes J, Lemke H, Baisch H, Wachter HH, Schwab U, Stein H. Cell cycle analysis of a cellular proliferation-associated human nuclear antigen defined by the monoclonal antibody Ki-67. *J Immunol* 1984;133:1710-1715.
11. Kim D, Gregory CW, Smith GJ, Mohler JL. Immunohistochemical quantitation of androgen receptor expression using color video image analysis. *Cytometry* 1999;35:2-10.
12. Kawamata N, Park D, Wilczynski S, Yokota J, Koeffler HP. Point mutations of the *Mxi-1* gene are rare in prostate cancers. *Prostate* 1996;29:191-193.
13. Buttyan R, Sawczuk IS, Benson MC, Siegal JD, Olsson CA. Enhanced expression of the c-myc protooncogene in high-grade human prostate cancers. *Prostate* 1987;11:327-337.
14. Grant AG, Flomen RM, Tizard ML, Grant DA. Differential screening of a human pancreatic adenocarcinoma λ gt11 expression library has identified increased transcription of elongation factor EF-1 alpha in tumour cells. *Int J Cancer* 1992;51: 740-745.
15. Tatsuka M, Mitsui H, Wada M, Nagata A, Nojima H, Okayama H. Elongation factor-1 α gene determines susceptibility to transformation. *Nature* 1992;359:333-336.
16. Feuer JA, Lush RM, Venzon D, Duray P, Tompkins A, Sartor O, Figg WD. Elevated carcinoembryonic antigen in patients with androgen-independent prostate cancer. *J Invest Med* 1998;46: 66-72.
17. Chen KS, DeLuca HF. Isolation and characterization of a novel cDNA from HL-60 cells treated with 1,25-dihydroxyvitamin D-3. *Biochim Biophys Acta* 1994;1219:26-32.
18. Nishiyama A, Matsui M, Iwata S, Hirota K, Masutani H, Nakamura H, Takagi Y, Sono H, Gon Y, Yodoi J. Identification of thioredoxin-binding protein-2/vitamin D3 up-regulated protein 1 as a negative regulator of thioredoxin function and expression. *J Biol Chem* 1999;274:21645-21650.
19. Yakirevich E, Naot Y. Cloning of a glucose phosphate isomerase/neuroleukin-like sperm antigen involved in sperm agglutination. *Biol Reprod* 2000;62:1016-1023.
20. Kim D, Gregory CW, French FS, Maygarden SJ, Smith GJ, Mohler JL. Androgen receptor expression during the transition from androgen-dependent to androgen-independent growth in the CWR22 prostate cancer xenograft. *Am J Pathol* 2002. 160:219-222.
21. Gregory CW, Johnson RT, Presnell SC, Mohler JL, French FS. Androgen receptor regulation of G1 cyclin and cyclin dependent kinase function in the CWR22 human prostate cancer xenograft. *J Andrology* 2001;22:537-548.
22. Gregory CW, He B, Johnson RT, Ford OH, Mohler JL, French FS, Wilson EM. A mechanism for androgen receptor-mediated prostate cancer recurrence after androgen deprivation therapy. *Cancer Res* 2001;61:4315-4319.
23. Culig Z, Hobisch A, Cronauer MV, Radmayr C, Hittmair A, Zhang J, Thurnher M, Bartsch G, Klocker H. Regulation of prostatic growth and function by peptide growth factors. *Prostate* 1996;28:392-405.
24. Scher HI, Sarkis A, Reuter V, Cohen D, Netto G, Petrylak D, Lianes P, Fuks Z, Mendelsohn J, Cordon-Cardo C. Changing pattern of expression of the epidermal growth factor receptor and transforming growth factor α in the progression of prostatic neoplasms. *Clin Cancer Res* 1995;1:545-550.
25. Sherwood ER, Van Dongen JL, Wood CG, Liao S, Kozlowski JM, Lee C. Epidermal growth factor receptor activation in androgen-independent but not androgen-stimulated growth of human prostatic carcinoma cells. *Brit J Cancer* 1998;77:855-861.
26. Putz T, Culig Z, Eder IE, Nessler-Menardi C, Bartsch G, Grunicke H, Uberall F, Klocker H. Epidermal growth factor (EGF) receptor blockade inhibits the action of EGF, insulin-like growth factor I, and a protein kinase A activator on the mitogen-activated protein kinase pathway in prostate cancer cell lines. *Cancer Res* 1999;59:227-233.
27. Gopalkrishnan RV, Su ZZ, Goldstein NI, Fisher PB. Translational infidelity and human cancer: role of the PTI-1 oncogene. *Int J Biochem Cell Biol* 1999;31:151-162.
28. Makino Y, Okamoto K, Yoshikawa N, Aoshima M, Hirota K, Yodoi J, Umesono K, Makino I, Tanaka H. Thioredoxin: a redox-regulating cellular cofactor for glucocorticoid hormone action. Cross talk between endocrine control of stress response and cellular antioxidant defense system. *J Clin Invest* 1996;98:2469-2477.
29. Hayashi S, Hajiro-Nakanishi K, Makino Y, Eguchi H, Yodoi J, Tanaka H. Functional modulation of estrogen receptor by redox state with reference to thioredoxin as a mediator. *Nucleic Acids Res* 1997;25:4035-4040.
30. Kroemer G, Zamzami N, Susin SA. Mitochondrial control of apoptosis. *Immunol Today* 1997;18:44-51.
31. Ueda S, Nakamura H, Masutani H, Sasada T, Yonehara S, Takabayashi A, Yamaoka Y, Yodoi J. Redox regulation of caspase-3(-like) protease activity: regulatory roles of thioredoxin and cytochrome C. *J Immunol* 1998;161:6689-6695.
32. Mustacich D, Powis G. Thioredoxin reductase. *Biochem J* 2000; 346:1-8.

Androgen Receptor Expression and Cellular Proliferation During Transition from Androgen-Dependent to Recurrent Growth after Castration in the CWR22 Prostate Cancer Xenograft

Desok Kim,* Christopher W. Gregory,^{†‡}
Frank S. French,*[†] Gary J. Smith,*[§] and
James L. Mohler*^{‡§}

From the Lineberger Comprehensive Cancer Center,* the Department of Pediatrics,[†] the Laboratories for Reproductive Biology,[‡] Department of Surgery, Division of Urology, and the Department of Pathology and Laboratory Medicine,[§] University of North Carolina, Chapel Hill, North Carolina

Androgen receptor expression was analyzed in the CWR22 human prostate cancer xenograft model to better understand its role in prostate cancer recurrence after castration. In androgen-dependent tumors, 98.5% of tumor cell nuclei expressed androgen receptor with a mean optical density of 0.26 ± 0.01 . On day 2 after castration androgen deprivation decreased immunostained cells to 2% that stained weakly (mean optical density, 0.16 ± 0.08). Cellular proliferation measured using Ki-67 revealed <1% immunostained cells on day 6. Androgen receptor immunostained cells increased to 63% on day 6 and 84% on day 32 although immunostaining remained weak. Cellular proliferation was undetectable beyond day 6 after castration until multiple foci of 5 to 20 proliferating cells became apparent on day 120. These foci expressed increased levels of prostate-specific antigen, an androgen receptor-regulated gene product. In tumors recurrent 150 days after castration androgen receptor-immunostaining intensity was similar to CWR22 tumors from intact mice although the percentage of cells immunostained was more variable. The appearance of proliferating tumor cells that expressed androgen receptor and prostate-specific antigen 120 days after castration suggests that these cells represent the origin of recurrent tumors. (*Am J Pathol* 2002, 160:219–226)

High-affinity binding of dihydrotestosterone to androgen receptor (AR) causes AR to function as a transcription factor^{1,2} that regulates a network of androgen response genes.^{3,4} Prostate cancer (CaP) is androgen-dependent and its growth is mediated by this AR-regulated gene network. Androgen deprivation causes reduced AR ex-

pression,⁵ apoptosis, decreased cell volume,⁶ and decline of serum prostate-specific antigen (PSA). However, most CaPs eventually develop the capacity for recurrent growth in the absence of testicular androgen. All of 22 specimens of testicular androgen-independent metastatic CaP showed positive immunohistochemical staining for AR protein.⁷ Transurethral resection of prostate specimens from 10 untreated CaP patients and 20 patients with CaP recurrent after androgen deprivation were compared and no significant difference in the percentage of AR-positive cells was found.^{8,9} Because AR expression is similar in androgen-dependent and recurrent CaP, we sought to understand how AR expression changes in relation to cellular proliferation in the interval between androgen deprivation and tumor recurrence.

CWR22 is an androgen-dependent human CaP xenograft propagated subcutaneously in nude mice. CWR22 resembles the majority of human CaPs; CWR22 secretes PSA, undergoes tumor regression after androgen deprivation, and recurs as a palpable, growing and ultimately lethal tumor after several months in the absence of testicular androgen.^{10–13} We demonstrated that recurrence of CWR22 tumor after androgen deprivation was associated with re-expression of a network of androgen-regulated genes including PSA, human kallikrein-2, *Nkx 3.1*, AR co-activator ARA-70, cell cycle genes *Cdk1* and *Cdk2*,³ and insulin-like growth factor binding protein-5.¹⁴ Recently, Amler and associates¹⁵ have reported incomplete reactivation of the androgen response pathway despite androgen absence in recurrent CWR22 using microarray analysis. Similar expression of AR and these androgen-regulated genes in androgen-dependent and recurrent CWR22 tumors suggested a role for AR regu-

Supported by the National Institutes of Health [grants RO1-AG-11343 (to F. S. F., J. L. M.), RO1-CA-64865 (to G. J. S., J. L. M.), P01-CA-77739 (to J. L. M., F. S. F., G. J. S.) and P30-HD-18968 (DNA and Tissue Culture Cores)], the United States Army Medical Research and Materiel Command (grant 98-1-8538 to J. L. M.), and the American Foundation for Urologic Disease and Merck U.S. Human Health (to C. W. G.).

D. K. and C. W. G. contributed equally to this work.

Accepted for publication October 8, 2001.

Address reprint requests to James L. Mohler, M.D., University of North Carolina, Division of Urology, CB# 7235, Chapel Hill, NC 27599-7235. E-mail: jmohler@med.unc.edu.

lation of gene expression in the development of recurrent CWR22 despite the absence of testicular androgen.

Video image analysis has been used to quantitate AR expression more precisely than visual scoring.^{16–19} We developed an automated method for measuring AR expression in individual cells that was used to demonstrate the dependence of AR protein levels on serum androgen levels in the CWR22 model.²⁰ In CWR22 tumor-bearing mice castrated for 6 days, AR mean optical density (MOD) decreased to 57% of levels in tumors from intact mice. After 72 hours of exogenous testosterone administration to 6-day castrated mice, AR MOD in CWR22 returned to the level found in tumors from intact mice. Cellular proliferation of testosterone-treated tumors reached ~50% of the original androgen-stimulated CWR22 tumors from intact mice.¹⁴ These data suggested that the majority of CWR22 cells on day 6 after castration had functional AR. In archived radical prostatectomy specimens, AR protein content was higher in androgen-dependent, clinically localized CaP and lower in prostate intraepithelial neoplasia than benign prostatic hyperplasia (BPH).^{19,20} AR immunostaining intensity was similar in androgen-stimulated and recurrent tumors from the CWR22 xenograft and transurethral resection of the prostate specimens of BPH; all tissues were small volume and fixed immediately after procurement.²⁰ Finally, 12 specimens of recurrent CaP and 16 specimens of BPH, all acquired by transurethral resection of the prostate and fixed immediately, exhibited similar AR immunostaining (unpublished data). Taken together, these findings suggest that AR is expressed in androgen-stimulated CaP, diminished but recoverable after castration, and re-expressed despite androgen absence on CaP recurrence.

We sought to test the hypothesis that re-expression of AR coincided with the onset of androgen-independent cellular proliferation in CaP. To test this hypothesis, the temporal relationship between AR protein expression and cellular proliferation was determined using the CWR22 xenograft model during tumor regression and recurrence after castration. Quantitative immunohistochemistry and color video image analysis were used to measure precisely the proportion of cells expressing AR and Ki-67 and the intensity of expression of AR associated with response to androgen deprivation and emergence of the recurrent phenotype.

Materials and Methods

Research Specimens

Nude/nude athymic mice were purchased from Harlan Sprague-Dawley, Inc., Indianapolis, IN. The CWR22 tumor model has been maintained by continuous passage since December of 1995 from CWR22 cells that were a gift from Thomas A. Pretlow, MD, PhD, Case Western Reserve University. CWR22 tumors were transplanted as 1 million dissociated cells suspended in Matrigel (Collaborative Biotech Inc., Bedford, MA) injected subcutaneously into nude mice 4 to 5 weeks of age.^{11,12} A 12.5-mg sustained-release testosterone pellet (Innovative Re-

search of America, Sarasota, FL) was placed subcutaneously in each animal 2 days before tumor injection and every 3 months thereafter to maintain consistent serum levels of testosterone of ~4 ng/ml. After tumors reached a volume of 1 cm³, animals were anesthetized with methoxyflurane, castrated, and the testosterone pellets removed. Intact mice bearing tumors and castrated animals with either regressed or recurrent CWR22 tumors were exposed to methoxyflurane and sacrificed by cervical dislocation. Tumor height, width, and depth were measured using calipers and tumor volume was calculated by multiplying these three measurements and 0.5234. Tumors were excised and cut into several pieces (~125 mm³); half was frozen in liquid nitrogen and half was fixed in 10% buffered formalin for 24 to 48 hours, washed in phosphate-buffered saline (PBS) for 24 hours, and paraffin-embedded. Specimens of BPH prepared identically were used as positive controls. Blood was obtained on sacrifice of all tumor-bearing mice for measurement of serum PSA.

Immunohistochemistry

The avidin-biotin-immunoperoxidase technique²¹ was modified for use in paraffin-embedded tissues that were immunostained using capillary action with a MicroProbe staining station (Fisher Scientific, Pittsburgh, PA).²² Monoclonal antibody (mAb) F39.4.1 (BioGenex, San Ramon, CA) recognizes an epitope in the N-terminal region of human AR.²³ mAb MIB-1 (Oncogene, Cambridge, MA) and polyclonal antibody MIB-5 (DAKO Corp., Carpinteria, CA) react with the cell cycle-associated antigen Ki-67 expressed during the proliferative phases (G₁, S, G₂, and M) but absent in the resting phase (G₀) of the cell cycle.²⁴ mAb A67-B/E3 (Santa Cruz Biotechnology, Inc., Santa Cruz, CA) corresponds to amino acids 1 to 261 representing full length PSA p30 of human origin.²⁵

Paraffin-embedded CWR22 tumor specimens were cut into 6- μ m-thick histological sections. After deparaffinization and rehydration, tissue sections were heated to 100°C for 30 minutes in a vegetable steamer in the presence of antigen retrieval solution (CITRA, pH 6.0; BioGenex) and cooled for 10 minutes. Slides were preincubated with 2% normal horse serum for 5 minutes at 37°C and washed with automation buffer (Fisher Scientific).

AR mAb was diluted 1:300 (0.13 μ g/ml in PBS containing 0.1% bovine serum albumin, pH 7.4) and sections were stained for 120 minutes at 37°C. Slides were incubated in biotinylated anti-mouse immunoglobulin (IgG) (Vector Laboratories, Inc., Burlingame, CA) for 15 minutes at 37°C (1:200 in PBS, pH 7.4) and in horseradish peroxidase-conjugated avidin-biotin complex (Vector Laboratories, Inc.) for 15 minutes at 37°C (1:100 in PBS, pH 7.4). The immunoperoxidase complexes were visualized using diaminobenzidine tetrahydrochloride (Vector Laboratories, Inc.) for 8 minutes at 37°C (0.75 mg/ml in Tris buffer containing 0.03% hydrogen peroxide, pH 7.6). Slides were dehydrated through graded alcohol solutions and cleaned by Hemo-De xylene substitute (Fisher Sci-

entific). Counterstaining was performed with hematoxylin (Gill's formula, 1:6 dilution; Fisher Scientific) for 12 seconds. Slides were mounted with Permount and coverslips. Two representative slides were selected from each time point and stained with the polyclonal AR antibodies, AR52 and PG-21, following protocols reported previously.^{5,26} AR52 was provided by Dr. Elizabeth M. Wilson (University of North Carolina at Chapel Hill) and PG-21 was provided by Dr. Gail S. Prins (University of Illinois at Chicago). Slides prepared from a CWR22 tumor on day 6 after castration and human BPH were included as external controls to avoid variation of immunostaining intensity caused during staining procedures. Nonimmune mouse IgG (Vector Laboratories, Inc.) was used instead of AR mAb at the same IgG concentration for negative control slides prepared from the same tissue blocks as specimens; negative control slides were nonreactive.

MIB-1 mAb staining was performed at an IgG concentration of 0.5 μ g/ml (1:50). All other steps were as described for AR immunostaining. Serial sections adjacent to the sections stained for AR were obtained from tumors on day 120 after castration and stained with MIB-1 mAb. Colon cancer tissue served as positive controls and 0.5 μ g/ml of nonimmune mouse IgG was used instead of MIB-1 mAb at the same IgG concentration for negative control slides prepared from the same tissue blocks as specimens; negative control slides were nonreactive.

PSA mAb (1:50, 4 μ g/ml) was biotinylated and blocked *in vitro* using the Iso-IHC kit (InnoGenex, San Ramon, CA) to avoid background staining caused by infiltrated murine cells in CWR22 tumors harvested from castrated animals. Sections were digested in Proteinase-K (20 μ g/ml, DAKO Corp.) for 6 minutes at room temperature. Sections were incubated in the blocking solution and labeled with PSA mAb for 1 hour at 37°C and in streptavidin-peroxidase (InnoGenex) for 5 minutes at 37°C. Immunoreaction was visualized by diaminobenzidine tetrahydrochloride for 8 minutes at 37°C. Double immunohistochemistry was performed on additional CWR22 slides to co-localize PSA expression among Ki-67-positive tumor cells. Sections were eluted by glycine buffer (pH 2.3) for 5 minutes three times at room temperature and antigen-retrieved as described previously. A mixture of normal goat serum (2%) and avidin (1:50 in PBS, Vector Laboratories, Inc.) was used for blocking for 5 minutes at 37°C. Sections were reacted with MIB-5 (1:50, 20 μ g/ml) mixed with biotin (1:50 in PBS, Vector Laboratories, Inc.) for 2 hours at 37°C. The same avidin-biotin-peroxidase complex technique used for MIB-1 was performed. Immunoreaction was visualized by 3-amino-9-ethylcarbazole (AEC) (Vector Laboratories, Inc.) for 10 minutes at 37°C. BPH and CaP specimens were used as positive controls. For the negative control slide, nonimmune rabbit IgG (Vector Laboratories, Inc.) was used instead of PSA mAb at the same IgG concentration; appropriate biotinylated IgGs were replaced with PBS in PSA and MIB-5 steps to check against cross-reactions. Negative control slides showed neither nonspecific reaction nor cross-reactions.

Automated Digital Image Analysis

Automated digital image analysis was performed as described previously.²⁰ Briefly, imaging hardware consisted of a Zeiss Axioskop microscope, a 3-chip charge-coupled device camera (C5810; Hamamatsu Photonics Inc., Hamamatsu, Japan), a camera control unit (Hamamatsu Photonics Inc.), and a Pentium-based personal computer. Each field of view for AR-stained slides was digitized at total magnification $\times 1200$ using a $\times 40$ objective (numerical aperture, 1.3). For MIB-1- and PSA-stained slides, a $\times 20$ objective (numerical aperture, 0.6) was used for total magnification at $\times 600$. Twenty images that contained ~ 200 to 250 nuclei at $\times 1200$ and 400 to 500 nuclei at $\times 600$ provided an adequate sample size for each tumor because the deviation of average intensity values of randomly chosen immunopositive areas became stable (within $\pm 5\%$).

Immunopositivity and immunonegativity were determined using a linear discriminant analysis based on hue, saturation, and intensity of 100 immunostained cells of an intact CWR22 specimen and 100 cells of a negative control slide, respectively. The positivity for AR, Ki-67, and PSA was defined as the total number of pixels from immunopositive areas divided by the total number of pixels from all nuclear areas detected in a given specimen.

Differences in MOD and percentage of AR-, Ki-67-, and PSA-positive cells from all images from all tumors at various time points were evaluated using Wilcoxon rank sum tests. Correlations between features were examined using the Pearson's product moment correlation test. *F*-tests were performed to compare the variances among samples. Statistical significance was achieved if $P < 0.05$.

Western Immunoblot Analysis of AR

Lysates were prepared from frozen CWR22 tumors. Tumor tissue (100 mg) was pulverized in liquid nitrogen, thawed on ice, and mixed with 1.0 ml of RIPA buffer with protease inhibitors (PBS, 1% Nonidet P-40, 0.5% sodium deoxycholate, 0.1% sodium dodecyl sulfate, 0.5 mmol/L phenylmethylsulfonyl fluoride, 10 μ mol/L pepstatin, 4 μ mol/L aprotinin, 80 μ mol/L leupeptin, and 5 mmol/L benzamidine). Tissue was homogenized on ice for 30 seconds using a Biohomogenizer (Biospec Products, Inc., Bartlesville, OK). Two μ l of 0.2 mol/L phenylmethylsulfonyl fluoride were added and homogenates incubated 30 minutes on ice. Homogenates were centrifuged at $10,000 \times g$ for 20 minutes; supernatants were collected and centrifuged to prepare final lysates. Supernatant protein (100 μ g) from each sample was electrophoresed in 12% sodium dodecyl sulfate-polyacrylamide gels and electroblotting to Immobilon-P membrane (Millipore Corp., Bedford, MA). Immunodetection used AR mAb F39.4.1 at 1:10,000 dilution. Secondary antibody (goat anti-mouse IgG conjugated to horseradish peroxidase; Amersham Corp., Arlington Heights, IL) was used for detection by enhanced chemiluminescence (DuPont-NEN Research Products, Boston, MA).

Table 1. Quantitation of Tumor Volume (cm³), AR Expression (AR MOD and %AR Positivity), Tumor Cellular Proliferation (%Ki-67 Positivity), and PSA Serum Levels (ng/ml) and Tissue Expression (%PSA Positivity) Measured in Androgen-Stimulated, Androgen-Deprived and Recurrent CWR22 Tumors*

Days after castration	No. of tumors	Tumor volume	AR MOD	%AR positivity	%Ki-67 positivity	Serum PSA	%PSA positivity
intact CWR22	12	1.11 ± 0.94 [†]	0.26 ± 0.01 [‡]	98.5 ± 0.2	73.5 ± 4.4	246.7 ± 55.3 [†]	17.4 ± 3.6
Day 1	2		0.15 ± 0.10	28.5 ± 7.4	56.9 ± 7.5		3.4 ± 1.0
Day 2	4	0.81 ± 0.09	0.16 ± 0.08	2.3 ± 5.5	26.1 ± 5.6	169.0 ± 53.7	5.5 ± 2.8
Day 4	2		0.11 ± 0.09	9.9 ± 8.6	9.4 ± 8.1		4.8 ± 1.1
Day 6	6	0.72 ± 0.49	0.15 ± 0.06	62.7 ± 4.8 [§]	0.8 ± 0.5	109.9 ± 76.3	5.6 ± 1.5
Day 12	6	0.81 ± 0.27	0.17 ± 0.06	70.9 ± 4.9 [§]	0.3 ± 0.3	18.8 ± 10.8	0.8 ± 0.9
Day 32	4	0.64 ± 0.25	0.17 ± 0.11	70.4 ± 7.3 [§]	0.1 ± 0.3	5.6 ± 4.1	0.6 ± 0.3
Day 64	2		0.15 ± 0.05	71.7 ± 12.2 [§]	0.4 ± 0.2		1.1 ± 0.1
Day 90	4	0.64 ± 0.30	0.17 ± 0.05	73.4 ± 6.5 [§]	0.8 ± 0.5	11.1 ± 1.8	1.5 ± 0.7
Day 120	4	0.78 ± 0.37	0.17 ± 0.03	72.3 ± 8.4 [§]	3.3 ± 1.2	21.3 ± 4.1	3.4 ± 0.1
Recurrent CWR22	12	1.63 ± 0.38	0.26 ± 0.01 [¶]	72.1 ± 7.6 [§]	49.1 ± 7.4 [¶]	261.5 ± 123.0 [¶]	7.2 ± 1.3 [¶]

*AR mean optical density (MOD), percent AR positivity, percent Ki-67 positivity, serum PSA level, and percent PSA positivity at all time points after castration decreased significantly ($P < 0.01$) compared to intact CWR22 except no significant differences were found for AR MOD in recurrent CWR22 and percent AR positivity on days 90 and 120 after castration compared to day 0 ($P > 0.05$).

[†]Tumor volume and serum PSA is described by mean ± SD and therefore the data for time points containing only two measurements were not presented.

[‡]The image analysis data for all nuclei for all tumors at each time point is described by mean ± SD. Each tumor is represented by 20 images containing 200 to 250 nuclei for AR and 400 to 500 nuclei for Ki-67.

[§]Percent AR positivity on days 6, 12, 32, 64, 90, and 120 after castration and upon recurrence increased significantly ($P < 0.001$) compared to days 1, 2, and 4 after castration.

[¶]Recurrent CWR22 showed a significant increase in AR MOD, percent Ki-67 positivity, serum PSA level, and percent PSA positivity compared to time points after castration ($P < 0.01$).

^{||}Serum PSA level and percent PSA positivity on day 120 after castration were significantly higher than on day 90 after castration ($P < 0.05$).

Results

Average MOD and percentage of cells expressing AR (percent AR positivity) were determined in tumors from CWR22-bearing mice before and after castration (Table 1). The majority of nuclei in CWR22 tumors from intact nude mice ($98.5 \pm 0.2\%$) showed intense staining of AR (MOD was 0.26 ± 0.01) (Figure 1). On day 1 after castration, AR MOD decreased and remained low on day 4 after castration whereas AR percent positivity declined to a minimum on day 2 (2%) and remained low on day 4 (10%). On day 6 after castration, AR-positive nuclei increased sixfold to 63% and were distributed evenly throughout all tumor sections. AR positivity increased further to 71% on day 12. AR MOD decreased to a low of 0.11 on day 4 and remained low at 0.15 to 0.17 on days 12 through 120 after castration. Recurrent CWR22 tumors obtained ~150 days after castration exhibited lower percent AR positivity ($72.1 \pm 7.6\%$) than CWR22 tumors from intact, androgen-stimulated mice ($P = 0.03$). However, among malignant nuclei expressing AR, MOD was similar ($P = 0.99$) in the original CWR22 under androgen stimulation and recurrent CWR22 in the absence of testicular androgens. Immunostaining of CWR22 tumors before and after castration yielded similar results when the polyclonal antibodies AR-52 and PG-21 were used instead of AR mAb F39.4.1 (data not shown). Western blotting (Figure 2) of CWR22 tumor lysates revealed similar AR levels in androgen-dependent and recurrent CWR22 tumors and reduced AR levels after castration until tumor recurrence.

The number of cells expressing Ki-67 in CWR22 tumors before and after castration were summarized in Table 1. Ki-67 positivity was high in CWR22 tumors from intact nude mice (Figure 1), decreased gradually on days

1 to 4 after castration, and remained at low or undetectable levels on day 6 through day 90 after castration. Although most CWR22 cells were in growth arrest, proliferating cells occurred randomly at a frequency $<1\%$ beyond day 6 until day 120 when multiple foci of 5 to 20 proliferating cells were detected throughout the tumors (Figure 1). Recurrent CWR22 tumors, compared to the original CWR22 tumors, exhibited lower cellular proliferation ($49.1 \pm 7.4\%$, $P = 0.006$). Mean serum PSA levels (261.5 ± 123.0 ng/ml) of mice bearing recurrent tumors ($n = 6$) increased to levels similar to those of tumor bearing intact mice (246.7 ± 55.3 ng/ml) (Table 1).

Foci of recurrent cellular proliferation, as indicated by Ki-67 staining, appeared on day 120 day after castration. When these proliferating foci were immunostained for PSA expression using double-staining immunohistochemistry, positive cytoplasmic staining for PSA was observed in the foci that contained Ki-67-positive cells (Figure 3). Moreover, the appearance of proliferating cells on day 120 after castration was associated with increased ($P = 0.01$) serum PSA levels (24 ± 3 ng/ml) compared to day 90 after castration (11 ± 2 ng/ml).

Recurrent CWR22 tumors showed more heterogeneous AR positivity, AR MOD, and Ki-67 positivity (Figure 4; A, B, and C) than CWR22 tumors from intact mice before castration (F -tests; $P < 0.001$, 0.05, and 0.05, respectively). Intertumor heterogeneity of cellular proliferation in recurrent CWR22 was reflected in serum PSA levels that ranged from 25 to 740 ng/ml when measured in recurrent tumor-bearing mice. Throughout the study period, AR MOD showed a parallel trend with Ki-67 positivity ($r = 0.64$, $P = 0.03$) and PSA levels ($r = 0.77$, $P = 0.02$) (Table 1). In addition, Ki-67 positivity was highly correlated with PSA levels ($r = 0.90$, $P = 0.002$).

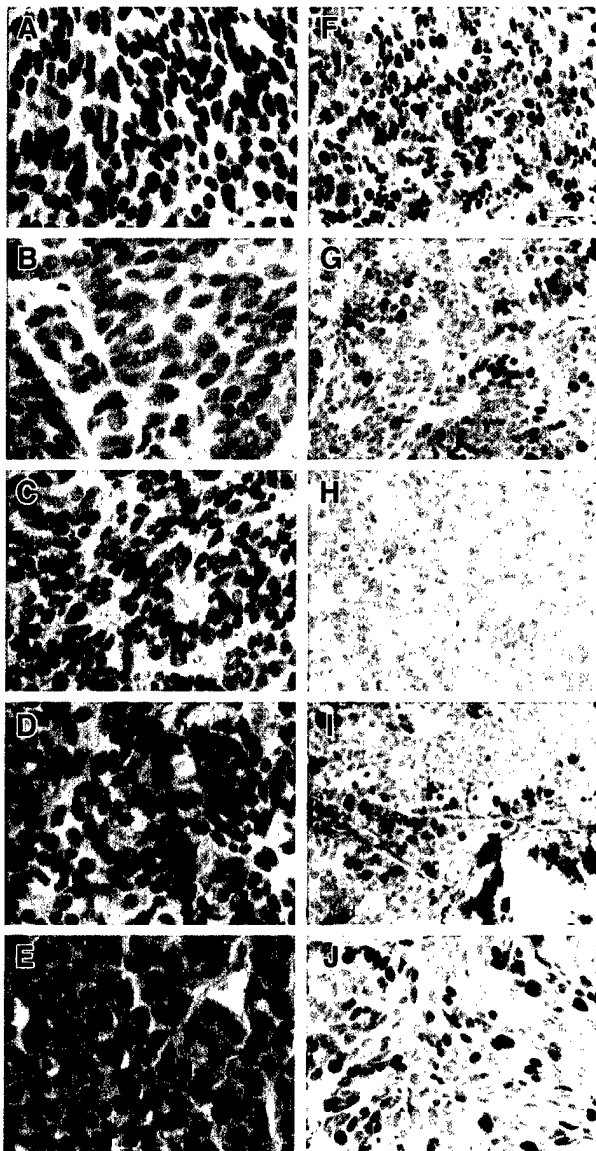


Figure 1. AR and Ki-67 immunohistochemistry of CWR22 tumors. AR expression was similar in androgen-dependent and recurrent tumors. AR-positive cells decreased to a minimum on day 2 after castration. Nuclear localization of AR returned on day 6 after castration but its intensity was lower than in androgen-dependent tumors. Higher percentages of AR-positive cells with lower levels of AR-staining intensity were recognized on days 32, 64, 90, and 120 after castration. **Left:** AR immunohistochemistry (scale bar, 10 μ m). **A:** CWR22 before castration. **B:** Day 2 after castration. **C:** Day 6 after castration. **D:** Day 120 after castration. **E:** Recurrent CWR22 ~150 days after castration. MIB-1 detection of the Ki-67 nuclear proliferation antigen showed similar rates of cellular proliferation in T-stimulated and recurrent tumors. Proliferation decreased on day 2 after castration and reached a level that was barely detectable on days 6 and 12 after castration. Proliferation was detectable as small nests of Ki-67-positive cells on day 120 after castration. **Right:** Ki-67 immunohistochemistry (scale bar, 20 μ m). **F:** CWR22 before castration. **G:** Day 2 after castration. **H:** Day 6 after castration. **I:** Day 120 after castration. **J:** Recurrent CWR22 ~150 days after castration.

Immunopositivity of PSA was highest in tumors from intact mice, decreased after castration, and remained low until sometime between 90 to 120 days after castration when an increase was noted within foci of proliferating cells. Immunopositivity of PSA was significantly correlated with AR MOD ($r = 0.658$, $P = 0.028$), Ki-67

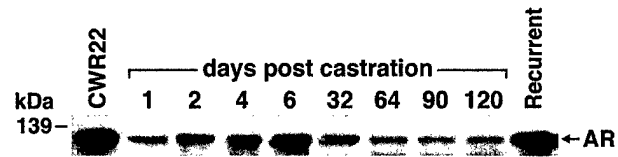


Figure 2. Western immunoblot analysis of AR protein in CWR22 tumors. An AR protein of 110 to 114 kD was present in lysates of androgen-dependent CWR22 tumors from intact mice. AR protein decreased after castration until tumor recurred ~150 days after castration. AR protein levels found in recurrent tumors in the absence of androgens were similar to those found in the original androgen-dependent tumors. The position of the molecular mass marker (kD) is indicated. This experiment was performed with two to six different tumors at each time point with similar results.

positivity ($r = 0.773$, $P = 0.006$), and serum PSA levels ($r = 0.818$, $P = 0.014$).

Discussion

In the present study, the temporal relationship between AR expression and cellular proliferation was investigated in CWR22 CaP xenografts during the transition from androgen-dependent to recurrent growth. Reduced AR protein immunostaining in CWR22 tumors after castration was similar to that observed in ventral prostates of castrated rats and mice.^{5,26,27} However, on day 6 after castration, percent AR positivity increased several fold and remained at higher levels on days 12, 32, 64, 90, and 120. Although AR was expressed in most nuclei, nuclear AR staining (MOD) remained relatively low throughout the period of tumor regression after castration. Proliferation of tumor cells ceased by day 6 after castration and remained at low to undetectable levels through day 90. Thus, during the period of tumor remission after androgen deprivation, nuclear AR levels were low and tumors

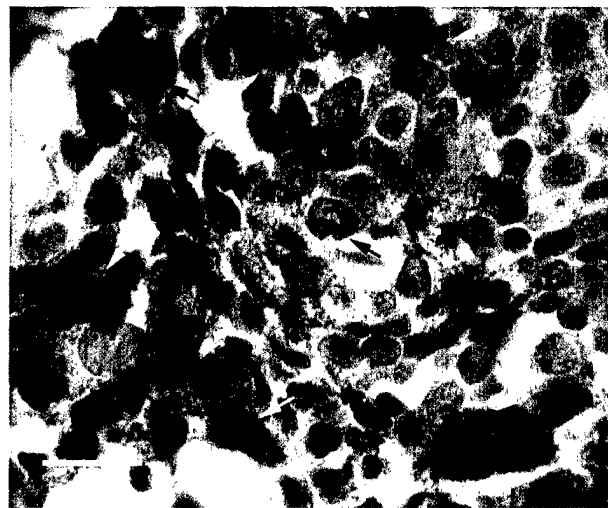


Figure 3. PSA and Ki-67 double immunohistochemistry of CWR22 tumors harvested from a mouse on day 120 after castration. Tissue PSA expression was visualized with diaminobenzidine tetrahydrochloride (cytoplasmic brown staining, **white arrows**) and Ki-67 expression was visualized with AEC (dark red nuclear staining, **black arrows**). Counterstaining was done with hematoxylin. Proliferating tumor cells emerged from the same foci where PSA was expressed (scale bar, 20 μ m). Ki-67 immunostaining from the double immunohistochemistry showed a pattern of numerous blobs in the nucleoplasm rather than a typical uniform nuclear staining. Protease treatment during PSA immunohistochemistry may have degraded Ki-67 protein.

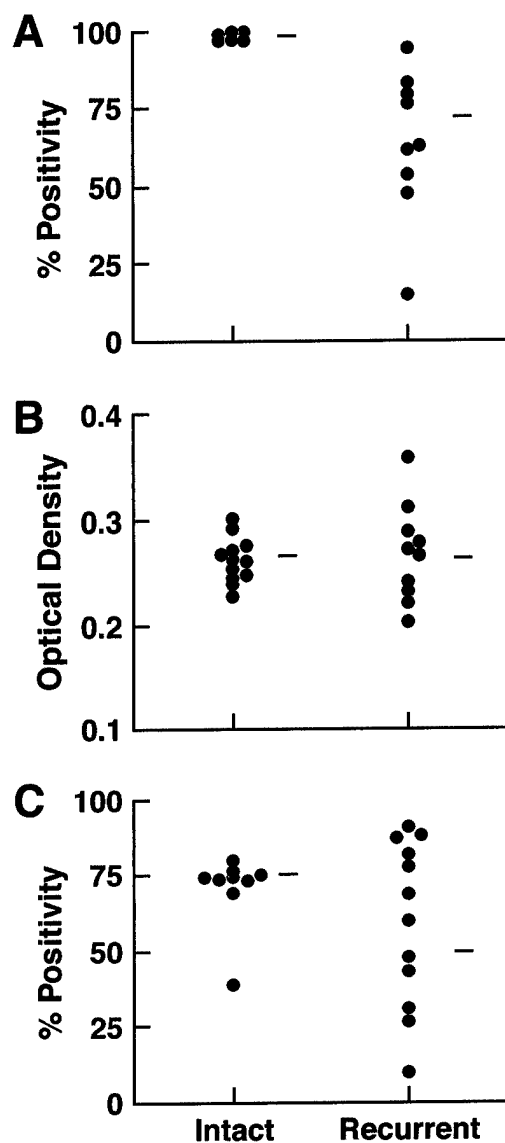


Figure 4. Comparison of heterogeneity of AR expression and Ki-67 expression in CWR22 specimens from intact mice and on recurrence ~150 days after castration. **A:** Mean percent AR positivity. **B:** MOD of AR. **C:** Mean percent Ki-67 positivity.

remained quiescent. Agus and associates²⁸ reported in their studies of cell-cycle regulators in the CWR22 xenograft that cellular proliferation assessed using Ki-67 and visual scoring fell to very low levels by day 10 after castration and remained so through day 30 after castration. The percentage of cells that stained intensely with AR mAb (F39.4.1) was low (10%) on days 3, 5, 7, and 10 after castration and reached the level of intact tumors by day 25 and thereafter. The difference between their and our reports may result from their dependence on visual scoring of AR immunostaining or their use of higher concentrations of AR mAb (2 μ g/ml) that may have increased nonspecific staining.²⁰

In recurrent tumors 150 days after castration, AR expression and cellular proliferation were more heterogeneous than in tumors from intact mice; recurrent tumors exhibited lower percent-positive nuclei and greater vari-

ation between tumors than CWR22 tumors from intact mice. However, among nuclei immunostained for AR, there was no difference in AR MOD between intact and recurrent tumors. Previous studies have established that AR activation subsequent to binding of androgen results in increased nuclear levels of AR,²⁹ homodimerization of AR,³⁰ and binding of AR to DNA sequences that function as enhancers for AR-induced transcriptional activation.^{1,2,31} The similar levels of AR expression in intact and recurrent tumors suggests that nuclear AR may be stabilized despite the absence of testicular androgen in recurrent CWR22 by a ligand-independent or synergistic mechanism. AR activation is linked closely to stabilization of AR protein; binding of androgen stabilizes AR causing it to have a slower rate of degradation.³² AR MOD, by its definition, represents a mean nuclear staining intensity relative to cytoplasm.²⁰ Therefore, increased AR MOD may reflect AR activation. Another possible mechanism of increased AR expression in recurrent CWR22 is AR gene amplification. AR gene amplification was detected in 7 of 23 cases of recurrent human CaP whereas none was detected before androgen-deprivation therapy.³³ However, AR gene amplification in recurrent CWR22 tumors was not detected using Southern blot analysis and competitive reverse transcriptase-polymerase chain reaction.³⁴

Because AR was expressed in a lower percentage of cells and at a lower MOD in those cells expressing AR on days 1 to 4 after castration and AR re-expression occurred on gross tumor recurrence, the temporal relationship between recovery of AR expression and the onset of cellular proliferation should provide insight into the role of AR in CaP recurrence after castration. On day 120 after castration, when recurrent tumor growth was indicated by increased serum PSA but tumor sites did not yet demonstrate growth grossly, small foci of tumor cells were recognized in harvested samples that immunostained for Ki-67 and expressed PSA. These findings suggested these foci were precursors of the recurrent CWR22 tumor that appears grossly ~150 days after castration. Two groups of investigators have reported on the relationship between serum PSA and tumor recurrence after castration in the CWR22 model. Serum PSA increase before gross tumor recurrence in the CWR22 model was reported first by Nagabhushan and associates.¹² The time course of these events cannot be compared to our results because they performed castration at higher tumor volumes. Agus and associates²⁸ castrated CWR22 tumor-bearing mice at tumor volumes similar to our studies. They reported increased serum PSA ~115 days after castration that preceded tumor recurrence recognized grossly ~20 days later. We reported previously that PSA is one of several known androgen-regulated genes whose mRNA was expressed at increased levels in recurrent CWR22 despite the absence of testicular androgen.³ In the current study, these RNA findings were confirmed by PSA protein quantitation at the tissue level. PSA is a well known androgen-regulated gene,^{35,36} however, other factors such as vitamin D³⁷ and transforming growth factor- β ³⁸ have been shown to be involved in transcriptional regulation of the PSA gene. One or more of

these same factors may also be an initiator of recurrent growth. Nonetheless, coincidental increased PSA serum levels and tissue expression and the recurrence of tumor cellular proliferation might be caused by the same mechanisms, one of which is reactivation of AR.

Understanding the mechanisms driving recurrent growth is one of the most important issues in CaP research.³⁹⁻⁴¹ Because AR is a growth-stimulating transcription factor in CaP, reactivation of AR in the absence of testicular androgen could be one of the molecular events that initiates cellular proliferation and leads to tumor recurrence. Several mechanisms have been proposed for activation of AR in the absence of testicular androgen. AR mutations that alter ligand specificity may influence tumor progression subsequent to androgen deprivation by making AR more responsive to adrenal androgens. CWR22 cells express a mutant AR (His 874 to Tyr) that has normal transcriptional activity in response to testosterone and dihydrotestosterone but has altered ligand specificity making it more sensitive to activation by adrenal androgens including dehydroepiandrosterone.¹³ Alternatively, a ligand-independent mechanism might cause transcriptional activation of AR. Protein kinase A and C modulators might activate AR in the absence of ligand by altering phosphorylation of AR⁴²⁻⁴⁵ or AR co-activators.^{46,47} Stimulation of PKA activity resulted in activation of the N-terminal domain of AR in LNCaP cells.⁴⁸ Transfected AR was reported to be activated by insulin-like growth factor I, epidermal growth factor, and keratinocyte growth factor in DU-145 cells and PSA was increased by insulin-like growth factor I in LNCaP cells.⁴⁹ Overexpression of HER-2/neu receptor tyrosine kinase was reported to increase expression of PSA and enhance growth in the androgen-dependent human CaP LAPC-4 xenograft.⁵⁰ These effects required AR expression and seemed to occur through cross-talk between the AR and HER-2/neu pathways. We reported recently that high-level expression, increased stability, and nuclear localization of AR in recurrent tumor cells were associated with increased sensitivity to the growth-promoting effects of dihydrotestosterone at concentrations as low as the femtomolar range.³⁴ Additionally, we have shown that high expression of transcriptional intermediary factor 2 and steroid receptor coactivator 1 in recurrent CaP increases AR transactivation in response to physiological concentrations of adrenal androgens or other steroids with affinity for AR.⁵¹ A single event or combination of events that affect AR function may lead to recurrent tumor growth in the absence of testicular androgen.

The re-expression of AR and known androgen-regulated genes in the 150-day recurrent CWR22^{3,14,15} suggests that AR reactivation has a role in stimulating recurrent tumor growth. AR MOD decreased after castration and failed to increase until sometime between 120 days after castration and gross tumor recurrence. At the 120-day time point, if proliferating cells exhibited increased AR MOD, their rarity would preclude detection because <5% of malignant cells were proliferating. Quantitation of antigens using double-staining immunohistochemistry is technically difficult; our attempts to measure AR expression in Ki-67-immunopositive *versus* immunonegative

cells have been unsuccessful thus far. However, if the small foci of tumor cells on day 120 after castration are precursors of recurrent tumors, direct comparison of AR, androgen-regulated gene products, and other molecules in these foci of cellular proliferation *versus* other regions of the tumor may be useful to evaluate specific mechanisms driving recurrent growth. Further study of this transition from androgen-dependent to androgen-independent growth in CWR22 may provide valuable insights into the mechanism of androgen-deprivation treatment failure in patients.

Acknowledgments

We thank Dr. Madhabananda Sar for technical advice on immunohistochemistry; Dr. Charles Bagnell for help with image registration; Patricia Magyar, Yeqing Chen, Gail Grossman, and Natalie Edmund for technical assistance; Dominic Moore and Dr. Michael Schell for statistical assistance; and Sidney Holdrege for assistance with manuscript preparation.

References

1. Quigley CA, De Bellis A, Marschke KB, el-Awady MK, Wilson EM, French FS: Androgen receptor defects: historical, clinical, and molecular perspectives. *Endocr Rev* 1995, 16:271-321
2. Roy AK, Lavrovsky Y, Song CS, Chen S, Jung MH, Velu NK, Bi BY, Chatterjee B: Regulation of androgen action. *Vitam Horm* 1999, 55: 309-352
3. Gregory CW, Hamil KG, Kim D, Hall SH, Pretlow TG, Mohler JL, French FS: Androgen receptor expression in androgen-independent prostate cancer is associated with increased expression of androgen-regulated genes. *Cancer Res* 1998, 58:5718-5724
4. Eid MA, Kumar MV, Iczkowski KA, Bostwick DG, Tindall DJ: Expression of early growth response genes in human prostate cancer. *Cancer Res* 1998, 11:2461-2468
5. Prins GS, Birch L: Immunocytochemical analysis of androgen receptor along the ducts of the separate rat prostate lobes after androgen withdrawal and replacement. *Endocrinology* 1993, 132:169-178
6. Kyprianou N, Isaacs JT: Activation of programmed cell death in the rat ventral prostate after castration. *Endocrinology* 1988, 122:552-562
7. Hobisch A, Culig Z, Radmayr C, Bartsch G, Klocker H, Hittmair A: Androgen receptor status of lymph node metastases from prostate cancer. *Prostate* 1996, 28:129-135
8. Ruizeveld de Winter JA, Jansen PJ, Sleddens HMEB, Verleun-Mooijman MCT, Trapman J, Brinkmann AO, Santerse AB, Schröder FH, van der Kwast TH: Androgen receptor status in localized and locally progressive hormone refractory human prostate cancer *Am J Pathol* 1994, 144:735-746
9. De Vere White RW, Myers F, Chi S-G, Chamberlain S, Siders D, Lee F, Stewart S, Gumerlock PH: Human androgen receptor expression in prostate cancer following androgen ablation. *Eur Urol* 1997, 31:1-6
10. Pretlow TG, Wolman SR, Micale MA, Pelley RJ, Kursh ED, Resnick MI, Bodner DR, Jacobberger JW, Delmoro CM, Giaconia JM: Xenografts of primary human prostatic carcinoma. *J Natl Cancer Inst* 1993, 85:394-398
11. Wainstein MA, He F, Robinson D, Kung H-J, Schwartz S, Giaconia JM, Edgehouse NL, Pretlow TP, Bodner DR, Kursh ED, Resnick MI, Seftel A, Pretlow TG: CWR22: androgen-dependent xenograft model derived from a primary human prostatic carcinoma. *Cancer Res* 1994, 54:6049-6052
12. Nagabhushan M, Miller CM, Pretlow TP, Giaconia JM, Edgehouse NL, Schwartz S, Kung HJ, de Vere White RW, Gumerlock PH, Resnick MI, Amini SB, Pretlow TG: CWR22: the first human prostate cancer xenograft with strongly androgen-dependent and relapsed strains both in vivo and in soft agar. *Cancer Res* 1996, 56:3042-3046
13. Tan J-A, Sharief Y, Hamil KG, Gregory CW, Zang D-Y, Sar M, Gu-

- merlock PH, deVere White RW, Pretlow TG, Harris SE, Wilson EM, Mohler JL, French FS: Dehydroepiandrosterone activates mutant androgen receptors expressed in the androgen-dependent human prostate cancer xenograft CWR22 and LNCaP cells. *Mol Endocrinol* 1997, 11:450-459
14. Gregory CW, Kim D, Ye P, D'Ercole AJ, Mohler JL, French FS: Androgen receptor up-regulates insulin-like growth factor binding protein-5 (IGFBP-5) expression in a human prostate cancer xenograft. *Endocrinology* 1999, 140:2372-2381
15. Amlier LC, Agus DB, LeDue C, Sapinosa ML, Fox WD, Kern S, Lee D, Wang V, Leysens M, Higgins B, Martin J, Gerald W, Dracopoli N, Cordon-Cardo C, Scher HI, Hampton GM: Dysregulated expression of androgen-responsive and nonresponsive genes in the androgen-independent prostate cancer xenograft model CWR22-R. *Cancer Res* 2000, 60:6134-6141
16. Sadi MV, Barrack ER: Image analysis of androgen receptor immunostaining in metastatic prostate cancer. Heterogeneity as a predictor of response to hormonal therapy. *Cancer* 1993, 71:2574-2580
17. Tilley WD, Lim-Tio SS, Horsfall DJ, Aspinall JO, Marshall VR, Skinner JM: Detection of discrete androgen receptor epitopes in prostate cancer by immunostaining: measurement by color video image analysis. *Cancer Res* 1994, 54:4096-4102
18. Prins GS, Sklarew JJ, Pertschuk LP: Image analysis of androgen receptor immunostaining in prostate cancer accurately predicts response to hormonal therapy. *J Urol* 1998, 159:641-649
19. Magi-Galluzzi C, Xu X, Hlatky L, Hahnfeldt P, Kaplan I, Hsiao P, Chang C, Loda M: Heterogeneity of androgen receptor content in advanced prostate cancer. *Mod Pathol* 1997, 10:839-845
20. Kim D, Gregory CW, Smith GJ, Mohler JL: Immunohistochemical quantitation of androgen receptor expression using color video image analysis. *Cytometry* 1999, 35:2-10
21. Sar M: Application of avidin-biotin complex technique for the localization of estradiol receptor in target tissues using monoclonal antibodies. *Techniques in Immunocytochemistry*, vol 3. Edited by GR Bullock, P Petrusz. New York, Academic Press, 1985, pp 43-54
22. Brigati DJ, Budgeon LR, Unger ER, Koebler D, Cuomo C, Kennedy T, Perdomo JM: Immunocytochemistry is automated: development of a robotic workstation based upon the capillary action principle. *J Histotechnol* 1988, 11:165-183
23. Zegers ND, Claassen E, Neelen C, Mulder E, van Laar JH, Vorhorst MM, Berrevoets CA, Brinkmann AO, van der Kwast TH, Ruizeveld de Winter JA, Trapman J, Boersma WJA: Epitope prediction and confirmation for the human androgen receptor: generation of monoclonal antibodies for multi-assay performance following the synthetic peptide strategy. *Biochim Biophys Acta* 1991, 1073:23-32
24. Gerdes J, Lemke H, Baisch H, Wachter HH, Schwab U, Stein H: Cell cycle analysis of a cell proliferation-associated human nuclear antigen defined by the monoclonal antibody Ki-67. *J Immunol* 1984, 133:1710-1715
25. Lundwall A: Characterization of the gene for prostate-specific antigen: a human glandular kallikrein. *Biochem Biophys Res Commun* 1989, 161:1151-1159
26. Sar M, Lubahn DB, French FS, Wilson EM: Immunohistochemical localization of the androgen receptor in rat and human tissues. *Endocrinology* 1990, 127:3180-3186
27. Takeda H, Nakamoto T, Kokontis J, Chodak GW, Chang C: Autoregulation of androgen receptor expression in rodent prostate: immunohistochemical and in situ hybridization analysis. *Biochem Biophys Res Commun* 1991, 177:488-496
28. Agus D, Cordon-Cardo C, Fox W, Drobnjak M, Koff A, Golde D, Scher H: Prostate cancer cell cycle regulators: response to androgen withdrawal and development of androgen independence. *J Natl Cancer Inst* 1999, 91:1869-1876
29. Zhou ZX, Sar M, Simental JA, Lane MV, Wilson EM: A ligand-dependent bipartite nuclear targeting signal in the human androgen receptor. *J Biol Chem* 1994, 269:13115-13123
30. Wong C, Zhou ZX, Sar M, Wilson EM: Steroid requirement for androgen receptor dimerization and DNA binding. Modulation by intramolecular interactions between the NH2-terminal and steroid-binding domains. *J Biol Chem* 1993, 268:19004-19012
31. Avellar MCW, Gregory CW, Power SGA, French FS: Androgen-dependent protein interactions within an intron-1 regulatory region of the 20-kDa protein gene. *J Biol Chem* 1997, 272:17623-17631
32. Zhou ZX, Lane MV, Kempainen JA, French FS, Wilson EM: Specificity of ligand-dependent androgen receptor stabilization: receptor domain interactions influence ligand dissociation and receptor stability. *Mol Endocrinol* 1995, 9:208-218
33. Visakorpi T, Hyytinen E, Koivisto P, Tanner M, Keinänen R, Palmberg C, Palotie A, Tammela T, Isola J, Kallioniemi OP: In vivo amplification of the androgen receptor gene and progression of human prostate cancer. *Nat Genet* 1995, 9:401-406
34. Gregory CW, Johnson RT, Mohler JL, French FS, Wilson EM: Androgen receptor stabilization in recurrent prostate cancer is associated with hypersensitivity to low androgen. *Cancer Res* 2001, 61:2892-2898
35. Young CY, Montgomery BT, Andrews PE, Qui SD, Bilhartz DL, Tindall DJ: Hormonal regulation of prostate-specific antigen messenger RNA in human prostatic adenocarcinoma cell line LNCaP. *Cancer Res* 1991, 51:3748-3752
36. Cleutjens KB, van Eekelen CC, van der Korput HA, Brinkmann AO, Trapman J: Two androgen response regions cooperate in steroid hormone regulated activity of the prostate-specific antigen promoter. *J Biol Chem* 1996, 271:6379-6388
37. Skowronski RJ, Peehl DM, Feldman D: Vitamin D and prostate cancer: 1,25 dihydroxyvitamin D3 receptors and actions in human prostate cancer cell lines. *Endocrinology* 1993, 132:1952-1960
38. Gleave ME, Hsieh JT, Wu HC, von Eschenbach AC, Chung LW: Serum prostate specific antigen levels in mice bearing human prostate LNCaP tumors are determined by tumor volume and endocrine and growth factors. *Cancer Res* 1992, 52:1598-1605
39. Koivisto P, Kolmer M, Visakorpi T, Kallioniemi OP: Androgen receptor gene and hormonal therapy failure of prostate cancer. *Am J Pathol* 1998, 152:1-9
40. Klocker H, Culig Z, Eder IE, Nessler-Menardi C, Hobisch A, Putz T, Bartsch G, Peterziel H, Cato ACB: Mechanism of androgen receptor activation and possible implications for chemoprevention trials. *Eur Urol* 1999, 35:413-419
41. Sadar MD: Androgen-independent induction of prostate-specific antigen gene expression via cross-talk between the androgen receptor and protein kinase: a signal transduction pathway. *J Biol Chem* 1999, 274:7777-7783
42. Ikonen T, Palmimo JJ, Kallio PJ, Reinikainen P, Janne OA: Stimulation of androgen-regulated transactivation by modulators of protein phosphorylation. *Endocrinology* 1994, 135:1359-1369
43. De Ruiter PE, Teuwen R, Trapman J, Dijkema R, Brinkmann AO: Synergism between androgens and protein kinase C on androgen-regulated gene expression. *Mol Cell Endocrinol* 1995, 110:51-56
44. Nazareth LV, Weigel NL: Activation of the human androgen receptor through a protein kinase A signaling pathway. *J Biol Chem* 1996, 271:19900-19907
45. Culig Z, Hobisch A, Hittmair A, Cronauer MV, Radmayr C, Zhang J, Bartsch G, Klocker H: Synergistic activation of androgen receptor by androgen and leutinizing hormone-releasing hormone in prostatic carcinoma cells. *Prostate* 1997, 32:106-114
46. Rowan BG, Weigel NL, O'Malley BW: Phosphorylation of steroid receptor coactivator-1. Identification of the phosphorylation sites and phosphorylation through the mitogen-activated protein kinase pathway. *J Biol Chem* 2000, 275:4475-4483
47. Rowan BG, Garrison N, Weigel NL, O'Malley BW: 8-bromo-cyclic AMP induces phosphorylation of two sites in SRC-1 that facilitate ligand-independent activation of the chicken progesterone receptor and are critical for functional cooperation between SRC-1 and CREB binding protein. *Mol Cell Biol* 2000, 20:8720-8730
48. Sadar MD, Hussain M, Bruchovsky N: Prostate cancer: molecular biology of early progression to androgen independence. *Endocr-Relat Cancer* 1999, 6:487-502
49. Culig Z, Hobisch A, Cronauer MV, Radmayr C, Trapman J, Hittmair A, Bartsch G, Klocker H: Androgen receptor activation in prostatic tumor cell lines by insulin-like growth factor-I, keratinocyte growth factor and epidermal growth factor. *Eur Urol* 1995, 27(Suppl 2):S45-S47
50. Craft N, Shostak Y, Carey M, Sawyers CL: A mechanism for hormone-independent prostate cancer through modulation of androgen receptor signalling by the HER-2/neu tyrosine kinase. *Nat Med* 1999, 5:280-285
51. Gregory CW, He B, Johnson RT, Ford OH, Mohler JL, French FS, Wilson EM: A mechanism for androgen receptor-mediated prostate cancer recurrence after androgen deprivation therapy. *Cancer Res* 2001, 61:4315-4319